UNIVERSIDAD NACIONAL AUTÓNOMA DE MÉXICO

PROGRAMA DE MAESTRÍA Y DOCTORADO EN INGENIERÍA

INGENIERÍA EN EXPLORACIÓN Y EXPLOTACIÓN DE RECURSOS NATURALES – INGENIERÍA DE YACIMIENTOS

DEVELOPMENT OF ANALYTICAL SOLUTIONS FOR THE STUDY OF OILS WITH NON-NEWTONIAN RHEOLOGY OF THE TYPE OF POWER-LAW AND BINGHAM-PLASTIC

TESIS

QUE PARA OPTAR POR EL GRADO DE:

MAESTRO EN INGENIERÍA

PRESENTA:

HÉCTOR ERICK GALLARDO FERRERA

TUTOR PRINCIPAL

DR. FERNANDO SAMANIEGO VERDUZCO

FACULTAD DE INGENIERÍA

CIUDAD UNIVERSITARIA, CD. MX. **ENERO, 2019**

JURADO ASIGNADO:

Presidente: Dr. Jorge Alberto Arévalo Villagrán

Secretario: Dr. Néstor Martínez Romero

Vocal: Dr. Fernando Samaniego Verduzco

1 er. Suplente: M.I. Alfredo León García

2 d o. Suplente: Dr. Teodoro Iván Guerrero Sarabia

UNIVERSIDAD NACIONAL AUTÓNOMA DE MÉXICO.
División de Estudios de Posgrado, Facultad de ingeniería.
Cd. Universitaria, Ciudad de México, México.

TUTOR DE TESIS:

Dr. Fernando Samaniego Verduzco

FIRMA

To my beloved parents, for their infinite support and advice.

Abstract

Due to the complexity of the heavy fraction in these fluids, cases have been reported in which the rheology of heavy and extra-heavy oil at reservoir does not correspond to the classic flow models used to estimate reserves and characterize the productivity parameters of the well-reservoir system. A natural consequence of this is that the production forecasting done with classic models does not correspond to the real behavior of the wells.

This research is centered in the development of analytical models that help to describe the radial-flow of heavy and extra-heavy oil with non-Newtonian rheologies of the type of a Power-law and Bingham-plastic fluids at reservoir. A new model to treat the power-law type fluids with a pseudo-skin factor is presented, as well as two new solutions for the transient-flow of a Bingham-plastic fluid. To validate the new models, synthetic data from numerical simulation studies was used. The obtained results were satisfactorily compared.

It is expected that the implementation of this models will improve the productivity analysis of wells, permitting an accurate study of these fluids, so that possible treatments can be precisely evaluated.

Acknowledgments

The author wishes to express appreciation to the following: to Fernando Samaniego, for the guidance and supervision that made the completion of this research possible; to the UNAM, for the opportunity of continuing learning and developing my academic concerns; to the CONACYT, for the financial assistance provided; to the all administrative and academic staff which made my studies an incredible process; and to all the endearing people that I have been able to meet and share moments.

Table of Contents

List of Figures and Tables

[This page was intentionally left blank]

Chapter 1

Introduction

The reserves of heavy oil in the world are estimated to be near to 7.5 billion barrels, reason for which the understanding and development of these reservoirs are necessary for satisfying the global energy demand in the next decades[1]. Heavy oils can be classified according to their density and viscosity as (**Fig. 1.1**):

- **Conventional Heavy Oils,** for fluids with lower densities than 21 °API, and viscosities between 10 and 100 cp.
- **Extra-Heavy Oils,** which are fluids with densities between 10 and 7 °API, and viscosities in a range of 100 and 10×10^3 cp.
- **Oil Tar and Bitumen,** which are fluids with lower densities than 7 °API, and higher viscosities than 10×10^3 cp.

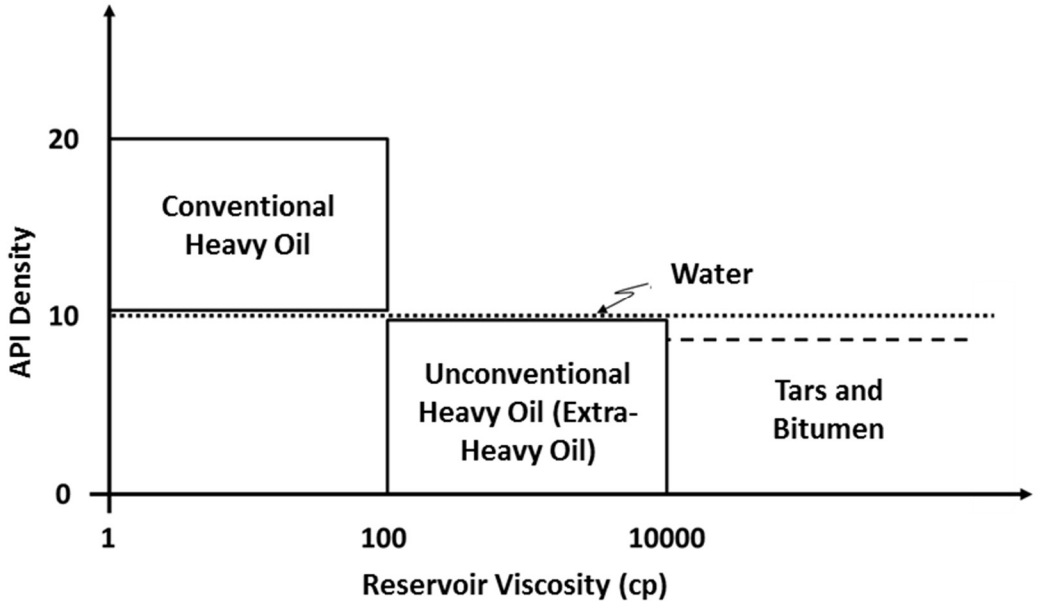

Figure 1. 1. Heavy oil classification (Modified from Benerjee[2]).

As a result of the formation environments, heavy oils possess a complex composition, which normally includes large amounts of asphaltenes, resins and other heavy molecules[3, 4, 5, 6] as well as low gas content. **Fig. 1.2** shows typical distributions of the asphaltene and resin content of some crude oils against its API density, it is seen that the quantity of C7-asphaltenes in high API-density crude oils is normally less than 1%, while in heavy and extra heavy oils, it may overtake values of 20% of its total mass.

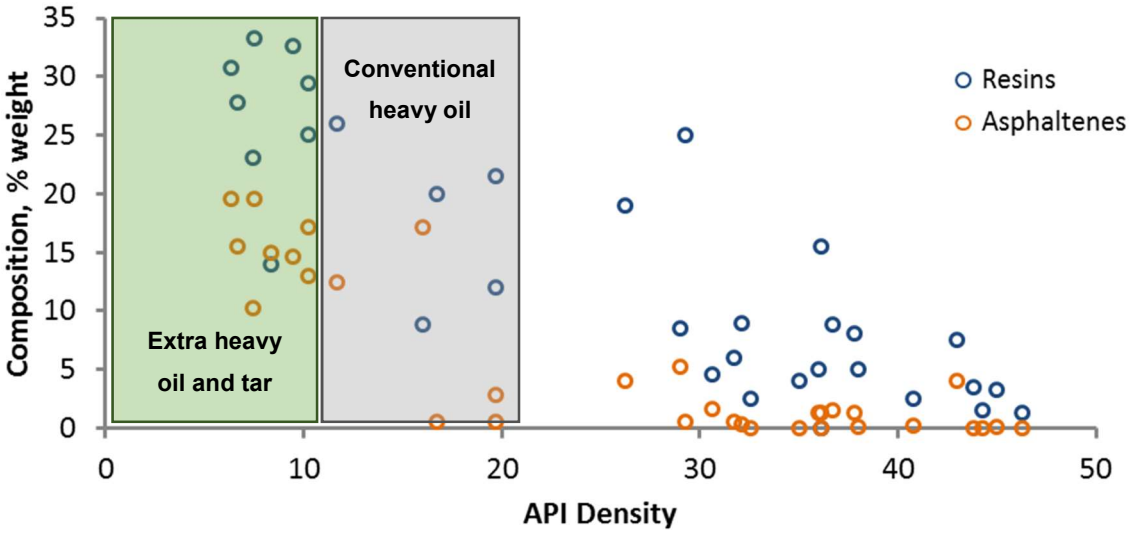

Figure 1. 2. Correlation between the API density and content of resins and asphaltenes for different oil mixtures[3, 4, 5].

The high content of asphaltenes in heavy and extra-heavy oil, as well as the presence of sand and metals, provoke several effects in its flow behavior, being some of them related with the existence of non-Newtonian rheologies. This research is conducted to understand and model the production mechanisms associated with rheologies of the type of power-law and Bingham plastic fluids.

Chapter 2

Literature review

Many heavy and extra heavy oil reservoirs around the world produce at higher rates than expected at primary conditions[6, 7, 8, 9, 10]. Regardless of the existence of several theories which try to explain this phenomenon, high production rates are mostly attributed to: non-Newtonian flow[11, 12, 13], solution-gas drive processes[14, 15, 16] and sand production effects[17, 18, 19, 20].

In this chapter, these theories are presented to clarify the state of the art and principal problems related to the production mechanisms in heavy and extra-heavy oils reservoirs.

2.1 Non-Newtonian Flow Behavior of Heavy Oil

Besides saturated and aromatic compounds, heavy and extra heavy oil systems contain several large and complex molecules; asphaltenes, resins and some metals (like vanadium and nickel) are found in these mixtures. As a result, the viscosity of these fluids has a wide range of values which spreads from 100 to over 10,000 cp, and some of them exhibit viscoelastic properties at reservoir conditions[11, 12, 13, 21].

Generally, for the problem of oil flow through a reservoir, the fluid is assumed to have a small and constant compressibility, a Newtonian viscosity and a laminar flow state (according to Darcy's model). However, it has been found that some heavy and extra heavy oil present a non-Newtonian behavior[22, 23, 24]. In these cases, the pressure drop in the Darcy equation can be correlated with the shear stress of a rheological model[16].

In this section, some flow models reported in the literature are presented.

2.1.1 Newtonian model

According to its rheological behavior, a Newtonian fluid exhibits a direct and constant proportionality between the exerted shear stress (τ) and its strain rate ($\dot{\gamma}$), as

$$\tau = \mu\dot{\gamma} \ , \quad \text{..... 2. 1}$$

where μ is named the dynamic viscosity.

The basic model to correlate flow velocity (v) as a result of a pressure drop (∇p) in a porous media with laminar state conditions is the Darcy equation[25], which indicates that these parameters are directly proportional to each other:

$$v = -\frac{k}{\mu}\nabla p \ , \quad \text{..... 2. 2}$$

being the mobility (k/μ) the adjusting factor in the relation.

Because of its simplicity, and since most of the reservoir fluids exhibit a Newtonian behavior, modified versions of this model are widely used to study wells productivity, as long as Newtonian viscosities exist.

2.1.2 Ostwald-de Waele model

There exist laboratory information which points that some heavy and extra-heavy oil reservoirs around the world exhibit a non-Newtonian Ostwald-de Waele (or power-law) behavior[11, 21, 26]. This model is defined by the next relation:

$$\tau = H\dot{\gamma}^n \ , \quad \text{..... 2. 3}$$

where n is the power-law index and H is called the consistence coefficient. In this case an apparent viscosity (μ_a) is used to study the resistance of the fluid to gradual deformation:

$$\mu_a = \frac{d\tau}{d\dot{\gamma}} = H\dot{\gamma}^{n-1} \quad . \quad \text{..... 2. 4}$$

For power-law fluids, the next analogous of the Darcy equation can be used[22, 27]

$$u^n = -\frac{k}{\mu_{eff}}\nabla p \ , \quad \text{..... 2. 5}$$

where the mobility is defined in terms of an effective viscosity (μ_{eff}):

$$\mu_{eff} = \frac{H}{12}(9 + 3/n)^n (150k\phi)^{(1-n)/2} \quad . \quad \text{..... 2. 6}$$

The applications found for this model are mainly focused on polymers, and some authors report its use to simulate the flow of heavy and extra-heavy oils[13, 24, 28].

2.1.3 Bingham plastic model

Some authors have reported that some heavy and extra heavy oil reservoirs require a minimum pressure drop to start production[11, 23, 29]. This corresponds to the description of a Bingham plastic fluid, which possess an internal structure that prevents the movement for values of shear stress less than a yield magnitude (τ_y), so the shearing movement only occurs when $\tau > \tau_y$. Once the deformation starts, these fluids exhibit a constant pseudo-viscosity (μ_B), so its rheological model is defined by the following expression

$$\tau = \tau_y + \mu_B\dot{\gamma} \quad . \quad \text{..... 2. 7}$$

At a macroscopic scale, the following transport equation can be used to model the flow of a Bingham plastic in the reservoir[22]

$$u = \begin{cases} -\frac{k}{\mu_B}\left(1 - \frac{G}{|\nabla p|}\right)\nabla p\ , & \text{for } |\nabla p| > G \\ 0\ , & \text{for } |\nabla p| \leq G \end{cases}\ , \quad \text{..... 2. 8}$$

where the parameter G accounts for the minimum pressure gradient required to start the flow, which is related with τ_y as:

$$G = \frac{\tau_y}{d}\ , \quad \text{..... 2. 9}$$

being d the characteristic pore size of the porous medium.

2.1.4 Herschel-Bulkley model

The Herschel-Bulkley (or modified power-law) model was developed as a generalization for time-independent non-Newtonian fluids[23], and it is given by

$$\tau = \tau_y + H\dot{\gamma}^{n-1}\ . \quad \text{..... 2. 10}$$

In this case, the following transport equation can be used to represent the flow velocity in the reservoir[30]

$$u^n = \begin{cases} \left(-\frac{k}{\mu_{eff}}\nabla p\right)\left[1 - \alpha\frac{G}{|\nabla p|}\right]^n\ , & \text{for } |\nabla p| > G \\ 0\ , & \text{for } |\nabla p| \leq G \end{cases}\ , \quad \text{..... 2. 11}$$

where μ_{eff} is

$$\mu_{eff} = 2H(1/n + 3)^n k^{1-n} r^{n-1}\ , \quad \text{..... 2. 12}$$

and α

$$\alpha = \frac{n + 4 + 1/n}{1 + 3n + 2n^2} \quad \text{.} \qquad \text{..... 2. 13}$$

2.1.5 Viscoelastic effects

It has been seen that some emulsions of bitumen with water possess a complex internal structure that rearranges with the exerted stress[13, 22, 27]. As consequence, the flowing phase exhibit viscoelastic properties in the porous media and its rheological behavior can be divided in regions, **Fig. 2. 1**: 1) a Newtonian flow region that exist at low flow velocities, 2) an intermediate power-law transition, and 3) a Newtonian flow region at high flow velocities. For the above, these fluids are named as power-law type[13, 31].

Depending on the behavior of the apparent viscosity, power-law type fluids can be classified as pseudo-plastic kind, if μ_a decreases with the flow velocity, and as dilatant kind, when μ_a increases with the flow velocity. Even though there exist rheological models to describe the complete behavior of power-law type fluids[13], for its simplicity, the use of time-independent coupled expressions is preferred for simulation purposes. However, the applications found are, as with purely power-law fluids, mainly focused on polymers.

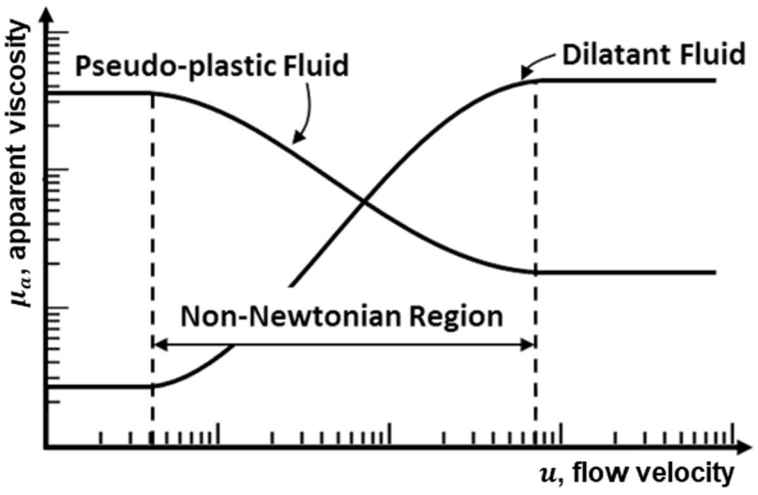

Figure 2. 1. Apparent viscosity for a power-law type fluid as a function of the flow velocity (after Poon and Kisman[13] and Bondor[31]).

2.2 Gas Drive Mechanisms in Heavy Oil Reservoirs

At conditions bellow the bubble point, depending on the depletion rate and viscous forces, heavy oils can act as super-saturated liquids, meaning that they have more dissolved-gas than they would at equilibrium. Hence, gas liberation does not start until a threshold-pressure is reached[32, 33].

Once the gas starts to evolve, it randomly forms micro-bubbles within the oil-phase[34, 35], and, as the capillary effects are inversely proportional to the size of bubbles, the flow of the gaseous phase may be delayed, and the critical saturation in the porous media will increase, enhancing the expansion mechanisms within the reservoir[36, 37].

In spite of this behavior, high-pressure gradients may cause viscous forces to prevail over the capillary effects[38, 39], and the tiny bubbles can be entrained by the viscosity of heavy oils. It has been observed that the simultaneous flow of the phases provides a "foamy" morphology to oil and improves the expansion mechanisms along the flow paths in the production system[40, 41, 42, 43].

2.3 Sand Production in Heavy Oil Reservoirs

Sand production is an induced phenomenon, which results from the drag viscous forces once the well is opened in unconsolidated formations[44]. As a result, the porous media acts as a plastic material until it reaches an elastic limit, after which fractures are formed. These fractures, better known as "wormholes," create flow channels of high permeability in the reservoir and enhance well's productivity[14, 45, 46].

Besides the changes in permeability and compaction of the system, sand production also improves the foamy oil formation processes[47, 48, 49, 50], and provides dilatant characteristics to the mixture[13]. Without sand production effects, the final recovery in several heavy oil reservoirs of Canada and Venezuela would be lower and unprofitable[51].

Chapter 3

Thesis statement

As the importance of unconventional resources has increased, considerable progress has been made in understanding the flow mechanisms associated with the production of heavy and extra heavy oils. Even when the influence of complex rheologies, gas drive processes and sand production was identified for these reservoir fluids, the literature review shows that commercial simulators do not have procedures to incorporate the non-Newtonian effects to evaluate the reservoir performance, and that the only way to match the calculated results with the production history is through the alteration of the permeability, saturation pressures or gas mobility, which not always permits accurate forecasts –mainly in low bubble point pressure and matrix consolidated systems.

This research is conducted to obtain analytical expressions and develop practical models to represent the effect of non-Newtonian flow in heavy and extra heavy oil reservoirs. For it, the following assumptions are considered:

1. The temperature is constant along the system, which is homogeneous and isotropic in its flow-properties.

2. The porous media is saturated by water and under-saturated oil, and the second is the only flowing phase in the system.

3. The system is formed by a central well producing at constant rate in a cylindrical reservoir, as shown in **Fig. 3. 1**. Hence, radial flow exist and it can be represented with the continuity equation as:

$$\frac{1}{r}\frac{\partial}{\partial r}(r\rho_o u) = -\frac{\partial}{\partial t}(\phi_{HC}\rho_o)\ , \qquad \text{..... 3. 1}$$

where ρ_o, u and ϕ_{HC} are the oil's density and velocity, and the hydrocarbon porosity, respectively.

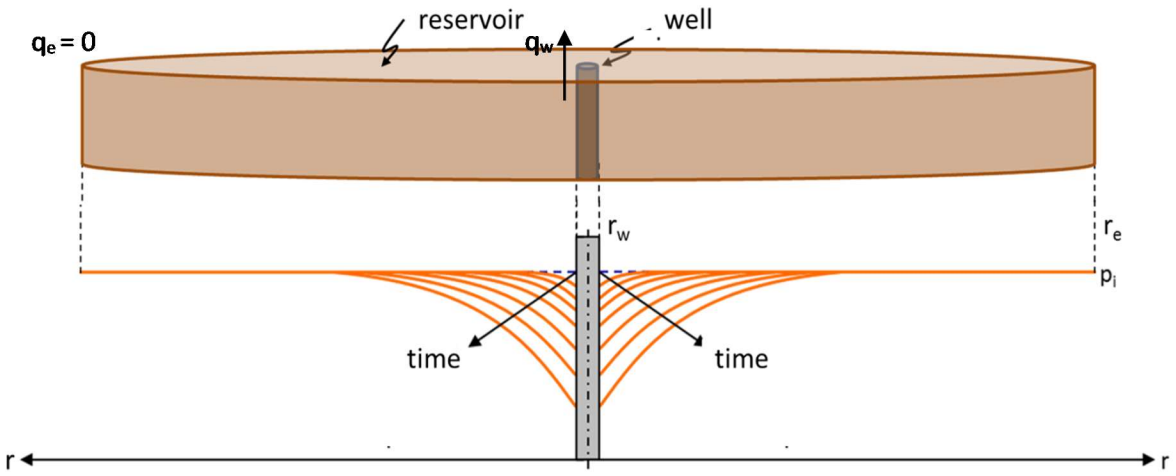

Figure 3. 1. Representation of the radial flow problem for a single well producing at constant rate q_w in a volumetric reservoir.

4. Oil is a slightly compressible fluid of constant compressibility, which equation of state is:

$$c_o = \frac{1}{\rho_o}\frac{\partial \rho_o}{\partial p}\ , \quad \text{.....} \quad 3.\ 2$$

and the porous media is also assumed to have a constant modified formation compressibility, which is modeled as

$$c_{\mathrm{F}}' = \frac{1}{\phi_{HC}}\frac{\partial \phi_{HC}}{\partial p}\ , \quad \text{.....} \quad 3.\ 3$$

so the total compressibility of the system is defined as:

$$c_t = c_o + c_F'\ . \quad \text{.....} \quad 3.\ 4$$

Chapter 4

Solutions for power-law type fluids

The power-law is the most widely used model to represent the flow of polymers and foams through a porous media. However, as discussed previously, some authors suggest its use in heavy and extra-heavy oil reservoirs[13, 24, 26]. For time-independent power-law fluids, the reference study was developed by Ikoku and Ramey[27], who derived a flow equation when substituting the modified Blake-Kozeny model (Eq. 2. 5) into the continuity equation (Eq 3. 1):

$$\frac{\partial^2 p}{\partial r^2}+\frac{n}{r}\frac{\partial p}{\partial r}=c_t\phi n\left(\frac{\mu_{eff}}{k}\right)^{1/n}\left(-\frac{\partial p}{\partial r}\right)^{1-\frac{1}{n}}\frac{\partial p}{\partial t}\ , \quad \text{..... 4. 1}$$

which was solved by the Laplace transform for the following conditions

$$p(r,t=0)=p_i\ , \quad \text{..... 4. 2}$$

$$q(r_w,t>0)=q_w\ , \quad \text{..... 4. 3}$$

$$p(r\to\infty,t>0)=p_i\ . \quad \text{..... 4. 4}$$

To generalize the solution, they proposed the following dimensionless groups:

$$p_{D_{NN}}=\frac{k}{\mu_{eff}r_w^{1-n}}\left(\frac{2\pi h}{qB}\right)^n(p-p_i)\ , \quad \text{..... 4. 5}$$

$$r_D=r/r_w\ , \quad \text{..... 4. 6}$$

$$t_{D_{NN}}=\frac{\eta_{NN}}{r_w^{3-n}}t\ , \quad \text{..... 4. 7}$$

where η is defined as:

$$\eta_{NN} = \frac{k}{\phi \mu_{eff} c_t n} \left(\frac{2\pi h}{qB} \right)^{n-1} . \quad \text{..... 4. 8}$$

Considering the above definitions, the Laplace solution for transient radial flow of a power law fluid in a homogenous reservoir is

$$\overline{\mathrm{P}}_{D_{NN}}(r_D, Z) = \frac{r_D^{\frac{1-n}{2}} K_{\frac{1-n}{3-n}} \left(\frac{2}{3-n} \sqrt{Z} r_D^{\frac{3-n}{2}} \right)}{Z^{3/2} K_{\frac{2}{3-n}} \left(\frac{2}{3-n} \sqrt{Z} \right)} , \quad \text{..... 4. 9}$$

where $\overline{\mathrm{P}}_{D_{NN}}$ is the dimensionless pressure-drop in the Laplace domain, Z is the Laplace variable, and K_v are K-Bessel functions of v order. Also, the following asymptotic approximation was obtained for Eq. 4. 9

$$p_{D_{NN}}(r_D = 1, t_D) = \frac{(3-n)^{\frac{2(n-1)}{3-n}}}{(1-n)\Gamma\left(\frac{2}{3-n}\right)} t_{D_{NN}}^{\frac{1-n}{3-n}} - \left(\frac{1}{1-n} \right) , \quad \text{..... 4. 10}$$

where $\Gamma(x)$ is the gamma function. The obtained expression was validated with a numerical simulator for an infinite reservoir based on the Douglas-Jhones method[52]. Later, the same authors extended their simulation models to contemplate the wellbore-storage and boundary dominated effects[53, 54]. Also, Ikoku presented a method for well-test interpretation in presence of non-Newtonian power-law fluids[55].

Besides the importance of the cited developments, since there exist different flow velocities through the reservoir, they are not useful for viscoelastic materials of power-law type. Hence, in this chapter a practical model, which is based in the definition of a pseudo-skin factor, is proposed for these fluids.

4.1 Conceptual frame of the skin factor

When studying pressure-production data with analytical or numerical models, the skin factor approach provides a simple mathematical tool to adjust the ideal formulations to a real measured response. In general, the total skin factor (S) is defined as the sum of the true formation damage (S_{tr}) with other skin effects (S_j) as

$$S = S_{tr} + \sum_{i=1}^{N} \lambda_j S_j \ , \quad \text{..... 4. 11}$$

where λ is a weight factor defined for each term in the sum. With the inclusion of the skin-factor, the real dimensionless pressure-drop ($p_{D_{real}}$) is defined as follows:

$$p_{D_{real}} = p_{D_{ideal}} + \mathrm{S} \ , \quad \text{..... 4. 12}$$

where $p_{D_{ideal}}$ is the ideal dimensionless pressure-drop.

Because the flow conditions change during the production, S is a time-dependent parameter[56]. However, as the skin-factor is assumed to change very slowly, it is normally considered as constant for punctual studies, and only as variable for long term simulations, in where S serves as a general tuning parameter for any change over time in the fluid or reservoir properties that is not contemplated by the analytical model.

4.2 Problem statement

The flow velocity and shear rate in a reservoir are related, and are proportional to the pressure gradient in the porous media. Hence, high velocities exist near the wellbore, where the bigger pressure-drop have place, and its magnitude blur as the radius advances into the reservoir. For power-law type fluids it means that, as a flow velocity distribution exist, the apparent viscosity has different behaviors along the system[13].

The **Fig. 4. 1** schematize the flow regions in a radial reservoir for power-law type fluids. As mentioned in **Chapter 2**, these materials exhibit power-law effects as a transition between two Newtonian sections of different viscosities (μ_{N_1} and μ_{N_2}, at high and low shear rates respectively). In consequence, the measured response of the system is expected to be affected[13]: for a pseudo-plastic kind behaving fluid (when n is less than one) the apparent viscosity is expected to increase as the pressure gradient extends on the reservoir. Hence, initially it would be easy to produce the fluids around the wellbore –because the shear rate in this zone is high–, but after a long period –when the drainage radius is bigger– the production would be more difficult and a larger pressure drop would be required to produce the fluids at a distance away from the wellbore. In this case, as the mobility is improved, and considering the definition of the skin factor, the non-Newtonian effect can be interpreted as a stimulation. In contrast, for a dilatant kind behaving fluid (when n is greater than one) the apparent viscosity would reduce as the pressure gradient extends into the reservoir, and the resulting behavior can be interpreted as an obstruction.

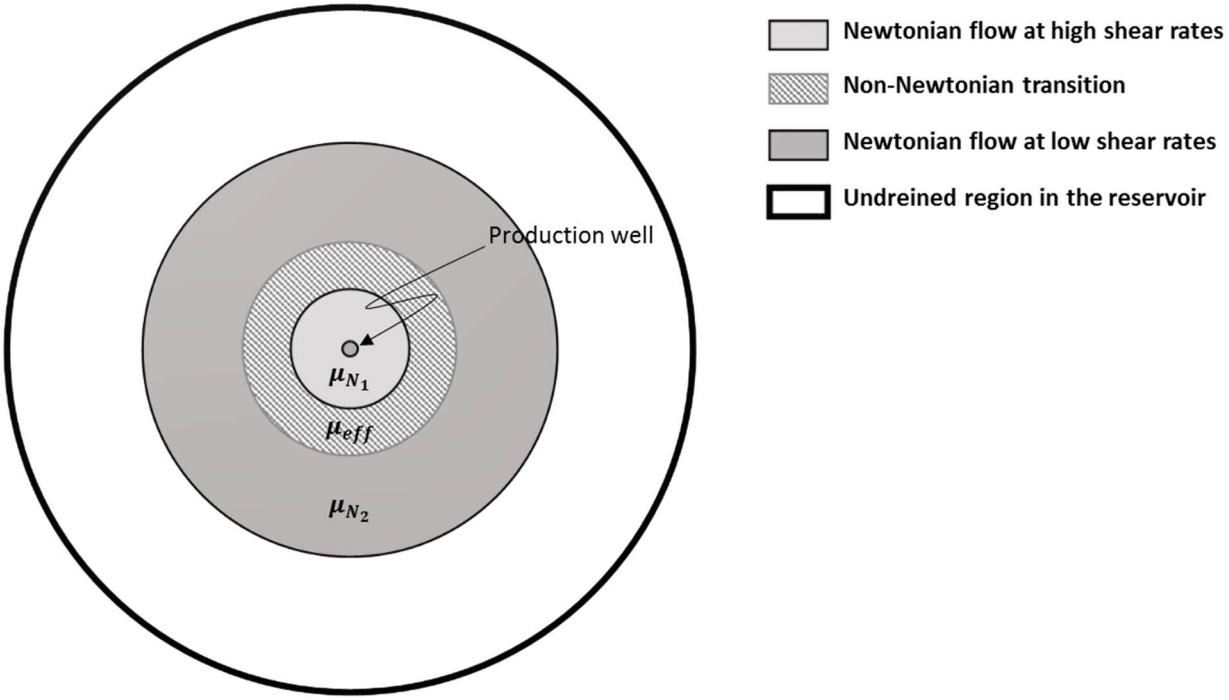

Figure 4.1. Flow regions in a radial reservoir for a power-law type fluid.

As the flow velocities are reasonably slow at the reservoir, in this work it is supposed that, for power-law type fluids, the Newtonian flow governs the production and that Non-Newtonian effects are restricted to a finite area within the porous media, as shown in **Fig. 6. 2**. Also, for the analysis, skin-factor is assumed as constant.

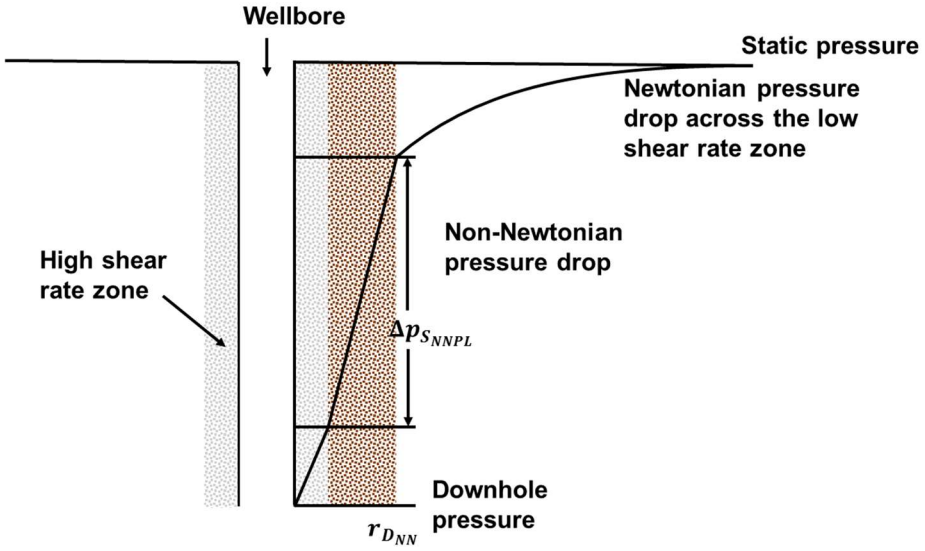

Figure 4. 2. Representation of the pressure drop behavior across the reservoir.

4.3 Formulation of a pseudo-skin factor for power-law type fluids

To include the effects of the power-law section, a steady state solution was used considering that this pressure drop has place in a limited section of the reservoir. Hence, the dimensionless form of the Eq. 4. 1 results in

$$\frac{d}{dr_D}\left(r_D^n \frac{dp_D}{dr_D}\right) = 0 \ , \quad \text{..... 4. 13}$$

which was solved for the following conditions

$$r_D \frac{dp_D}{dr_D}(r_D = 1) = -1 \ , \quad \text{..... 4. 14}$$

$$p_D\left(r_D = r_{D_{NN}}\right) = 0 \ , \quad \text{.....} \quad 4.\ 15$$

where $r_{D_{NN}}$ is the dimensionless radius of influence of the non-newtonian power-law effects. The resulting solution at the wellbore is:

$$p_D(r_D = 1) = -\frac{\left[r_{D_{NN}}^{1-n} - 1\right]}{1-n} \ , \quad \text{.....} \quad 4.\ 16$$

or in terms of normal variables:

$$p_{in} - p_w = \left(\frac{qB}{2\pi h}\right)^n \frac{\mu_{eff}}{k} \frac{[r_{NN}^{1-n} - r_w^{1-n}]}{1-n} \ . \quad \text{.....} \quad 4.\ 17$$

Now, defining the pressure drop at the non-newtonian skin zone as

$$\Delta p_{S_{NN}} = \Delta p_w^{NN} - \Delta p_w^{ideal} = \frac{qB\mu}{2\pi kh} S_{NN} \ , \quad \text{.....} \quad 4.\ 18$$

where S_{NN} is the pseudo-skin factor, and Δp_w^{ideal} is defined with a steady state solution:

$$\Delta p_w^{ideal} = \frac{qB\mu}{2\pi kh} \ln\left|\frac{r_{NN}}{r_w}\right| \ . \quad \text{.....} \quad 4.\ 19$$

Now combining Eq. 4. 17 and 4. 19 in 4. 18

$$\Delta p_{s_{NN}} = \left(\frac{qB}{2\pi h}\right)^n \frac{\mu_{eff}}{k} \frac{[r_{NN}^{1-n} - r_w^{1-n}]}{1-n} - \frac{qB\mu}{2\pi kh} \ln\left|\frac{r_{NN}}{r_w}\right| \ , \quad \text{.....} \quad 4.\ 20$$

or in terms of the pseudo-skin factor

$$S_{NN} = \left(\frac{qB}{2\pi h}\right)^{n-1} \frac{\mu_{eff}}{\mu} \frac{[r_{NN}^{1-n} - r_w^{1-n}]}{1-n} - \ln\left|\frac{r_{NN}}{r_w}\right| \ . \quad \text{.....} \quad 4.\ 21$$

In Eq. 4. 21, a negative value of S_{NN_P} would be characteristic of pseudo-plasticity, a positive one of dilatancy, and zero would correspond to an entirely Newtonian regime.

Chapter 5

Solutions for Bingham plastic fluids

The flow of asphaltene-rich oils in porous reservoirs may involve the presence of an initial pressure gradient[22], which has been associated with a reduction of the oil recovery and with the formation of stagnation areas within the reservoir. To represent the flow of this materials, the Bingham plastic model has been suggested[11, 22, 23], for which the following flow equation was derived by Wu et al.[57] when substituting the Mirzadjanzade model (Eq. 2. 8) into the continuity equation (Eq 3. 1):

$$\frac{\partial^2 p}{\partial r^2}+\frac{1}{r}\frac{\partial p}{\partial r}-\frac{G}{r}=\frac{1}{\eta_B}\frac{\partial p}{\partial t}\ , \quad \text{..... 5. 1}$$

where

$$\eta_B=\frac{k}{\phi\mu_B c_t}\ . \quad \text{..... 5. 2}$$

A solution for the Eq. 5. 1 was found by the authors for the following conditions with a polynomial approach based on the integral method

$$p(r,t=0)=p_i\ , \quad \text{..... 5. 3}$$

$$q(r_w,t>0)=q_w\ , \quad \text{..... 5. 4}$$

$$p(r\to\infty,t>0)=p_i\ . \quad \text{..... 5. 5}$$

To validate their results, as no analytical solution exist, the line-source solution (Theis equation) was used for the special case of $G=0$. Also a numerical simulator was developed.

In this chapter, dimensionless groups are proposed to generalize the Wu's solution for the Bingham plastic fluid problem. Also, analytical solutions where obtained by the Laplace transform method and a numerical model was developed to validate them. Finally, a method is proposed to approximately estimate the value of the minimum pressure drop at reservoir conditions.

5.1 Problem statement

The flow of a Bingham plastic can be practically understood as the superposition of two conditions: the transport of the pressure drop in the porous media and the flow below the threshold flow gradient (G). As shown in **Fig. 5.1**, there exist a zone between the boundaries of the named conditions in which the fluids remain static (as if it has an infinite viscosity, μ_∞); and in the zone where $\Delta p < G$, the flow resembles to the Newtonian case with a viscosity of μ_B, which is assumed constant for the following analysis.

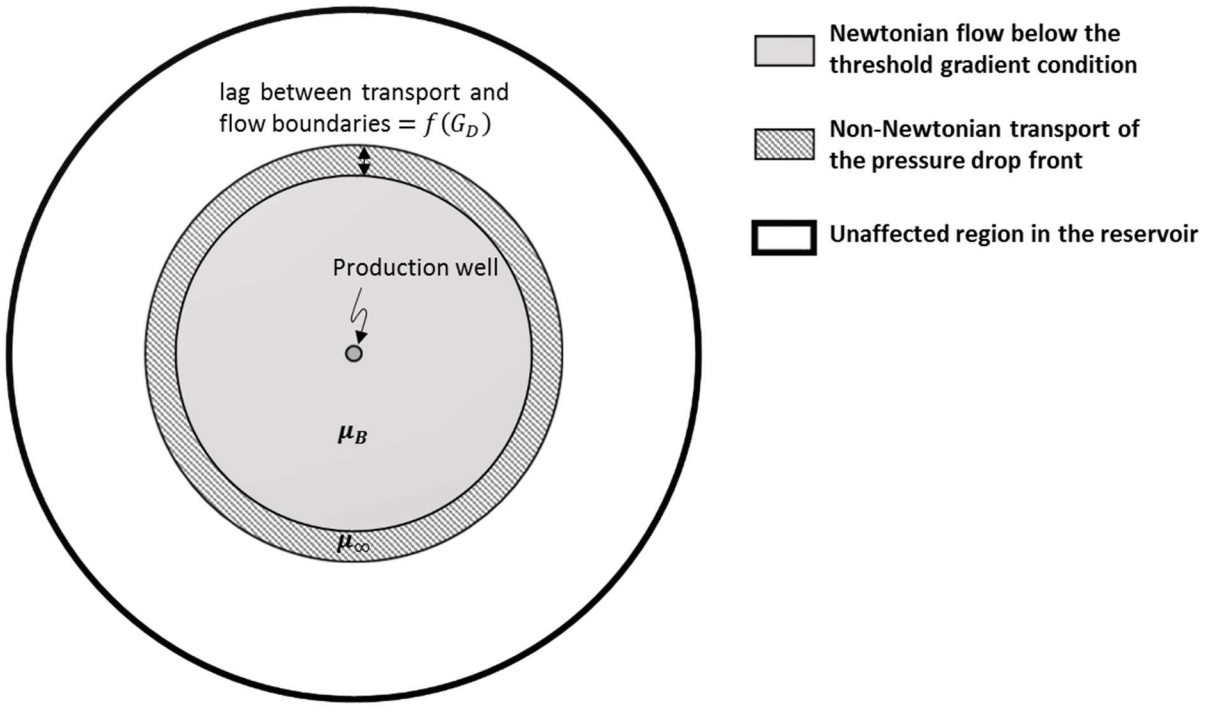

Figure 5.1. Flow regions in a radial reservoir for a Bingham plastic fluid.

5.2 Dimensionless variables

To generalize the resulting models, in this work the following groups are proposed:

$$p_{D_{NN}} = \frac{2\pi kh}{qB\mu_B}(p_i - p) \ , \quad \text{..... 5. 6}$$

$$r_D = \frac{r}{r_w} \ , \quad \text{..... 5. 7}$$

$$t_{D_{NN}} = \frac{\eta_B}{r_w^2} t \ , \quad \text{..... 5. 8}$$

$$G_D = \frac{2\pi khr_w}{qB\mu_B} G \ . \quad \text{..... 5. 9}$$

5.3 Transient flow solutions

Considering the aforementioned dimensionless groups, the Eq. 5. 1 is rewritten as

$$\frac{\partial^2 p_{D_{NN}}}{\partial r_D^2} + \frac{1}{r_D}\frac{\partial p_{D_{NN}}}{\partial r_D} + \frac{G_D}{r_D} = \frac{\partial p_{D_{NN}}}{\partial t_{D_{NN}}} \ , \quad \text{..... 5. 10}$$

and the considered boundary conditions, with $v = v_r + (k/\mu_B)G$, are

$$p_{D_{NN}}(r_D, 0) = 0 \ , \quad \text{..... 5. 11}$$

$$\left(r_D \frac{\partial p_{D_{NN}}}{\partial r_D}\right)_{r_D=1} = -1 \qquad t_{D_{NN}} > 0 \ , \quad \text{..... 5. 12}$$

$$p_{D_{NN}}(r_D \to \infty) = 0 \qquad t_{D_{NN}} > 0 \ . \quad \text{..... 5. 13}$$

Wu's polynomial approach is obtained as a solution for the above problem, and is

expressed in terms of dimensionless variables as follows:

$$p_{D_{NN}}(r_D = 1, t_{D_{NN}}) = G_D \delta(t_{D_{NN}}) - 2\Theta \ln\left|\frac{2}{\Omega} - \frac{1}{\Omega^2}\right| , \quad \text{..... 5. 14}$$

where $\Omega = 1 + \delta(t_{D_{NN}})$, $\Theta = [1 + 2\,\delta(t_{D_{NN}})]/4\delta(t_{D_{NN}})$ and $\delta(t_{D_{NN}})$ is the dimensionless penetration distance of the wellbore stimulus into the reservoir, which can be known from:

$$t_{C_{D_{NN}}} = G_D\left[\frac{\Omega^3}{6} - \frac{\Omega}{2} + \frac{1}{3}\right] + \frac{\Theta}{\Omega}\left[3\Omega - 1 - \ln|\Omega^4| - \frac{1}{\Omega} + \left(\frac{1}{\Omega} - 4\Omega\right)\ln\left|\frac{2}{\Omega} - \frac{1}{\Omega^2}\right|\right] . \quad \text{.. 5. 15}$$

In Eq. 5. 15, $t_{C_{D_{NN}}}$ is presented as a material balance time, as

$$t_{C_{D_{NN}}} = \eta_B t_C / r_w^2 = (\eta_B / r_w^2) \times (Q_p B_i / qB) , \quad \text{..... 5. 16}$$

where Q_p is the cumulative production.

In this work, the following two solutions where obtained (as shown in **Appendix A**) for the transient flow of a Bingham plastic fluid

$$p_{D_{NN}}(r_D = 1, t_D) = -\frac{1}{2}E_i\left(-\frac{0.25}{t_{D_{NN}}}\right) + \frac{1}{2}\ln|1 - G_D| + G_D[1 + \delta(t_{D_{NN}})] , \quad \text{..... 5. 17}$$

$$p_{D_{NN}}(r_D = 1, t_D) = -\frac{1}{2}E_i\left(-\frac{0.25}{t_{D_{NN}}}\right) + G_D\delta(t_{D_{NN}})\omega , \quad \text{..... 5. 18}$$

where $\omega = 0.0019\ln|t_{D_{NN}}|^2 - 0.0072\ln|t_{D_{NN}}| + 0.6173$.

To model the penetration distance, the steady-state solution of this problem was used and compared with Eq. 5. 17. The resulting Expression is

$$\delta(t_{D_{NN}}) = \sqrt{(1 - G_D)t_{D_{NN}}\exp(0.8091 + 2G_D)} , \quad \text{..... 5. 19}$$

which for Newtonian fluids results in the classical radius of investigation formula:

$$\delta\left(t_{D_{NN}}\right) = 4\sqrt{t_D} \ . \quad \text{..... 5. 20}$$

The full development of Eq. 5.19 is presented in **Appendix B**. In general, it has been seen that Eq. 5. 20 results in a good approximation for Bingham plastic fluids with values of G_D between 0 and 1.

Since G_D is inversely proportional to the production rate, it is important to note that the flow conditions are favored as the value of the initial pressure drop is greater. Also, permeability has been found to minimize the effect of G_D over production.

Chapter 6

Validation and use of the models

In this chapter, the previews models are used and validated. For the power-law type fluids, synthetic was analyzed; and for the Bingham plastic fluids, other published models and a simulator were used.

6.1 Power-law type fluids

For this case, synthetic data from a composite radial model, originally stablished for an injection problem[65], was used within the developed framework. The simulated system, **Figure 6.1**, is a two zones composite reservoir of different viscosities with homogenous permeability and porosity. The analyzed scenarios are detailed as follows.

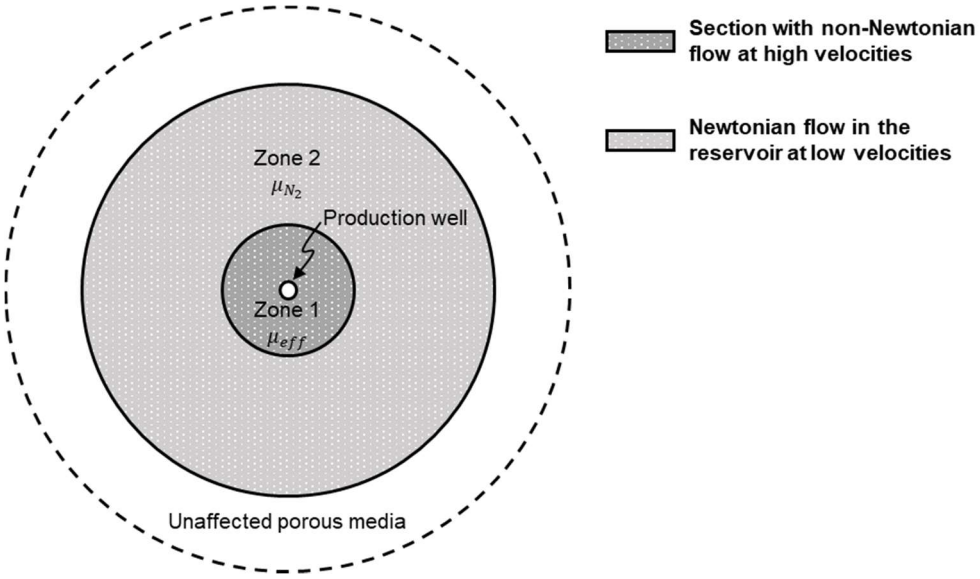

Figure 6.1. Representation of the simulated model for a power-law type fluid.

6.1.1 Pseudo-plastic type fluid

In this case a pseudo-plastic type fluid was analyze. The properties of this system, initially reported by Lund and Ikoku (1981), are indicated in **Table 6. 1**, considering for the simulation a constant radius of influence, for the power-law behavior, of $r_{D_{NN}} = 400$ and no wellbore storage effects.

Table 6. 1. Obtained values of the pseudo-skin factor for power-law type fluids.

r_w, m	0.1	k, md	100
h, m	5	$q, m^3/s$	5.5204×10^{-4}
$\phi, fraction$	0.2	c_t, Pa^{-1}	1×10^{-9}
r_{NN}, m	40	$H, N\cdot s^n/m^2$	0.003
n	0.6	$\mu_n, Pa\cdot s$	0.003

Figures 6.2 and 6.3 present the diagnostic and semi-log plots for the analyzed problem. The diagnostic plot shows two recognizable behaviors, the first (from 10 to 10^4 s) corresponds to the radial flow of a power-law fluid, and the second, to the late-radial flow of a Newtonian fluid. From the first part of this graph, a slope of 0.1718 can be identified in Δp and $Der\,\Delta p$ curves, which can be interpreted with the method proposed by Ikoku and Ramey (1979), resulting in a value of $n = 0.622$, corresponding with the input value of $n = 0.6$. Also, the late part of the derivative stabilizes in value of 296634 Pa, from which a permeability of 100 md was interpreted by the classical methods.

On the other hand, the semi-log plot shown a slope of $6.17 \times 10^5\ Pa\ /\ cycle$ and a value of Δp_w at 1 second of $3.17 \times 10^6\ Pa$, for which a permeability of 100 md and a total skin factor of -4.11 were estimated. Now, the developed model in Eq. 4.21 was used to compare with the results of the simulation, ($\mu_{eff} = 6.02 \times 10^{-6}\ N\cdot s^{0.6}\ /\ m^{1.6}$, Eq. 2.6). The skin factor obtained with Eq. 4.21 was of -4.4, which matches adequately with the previous interpreted value.

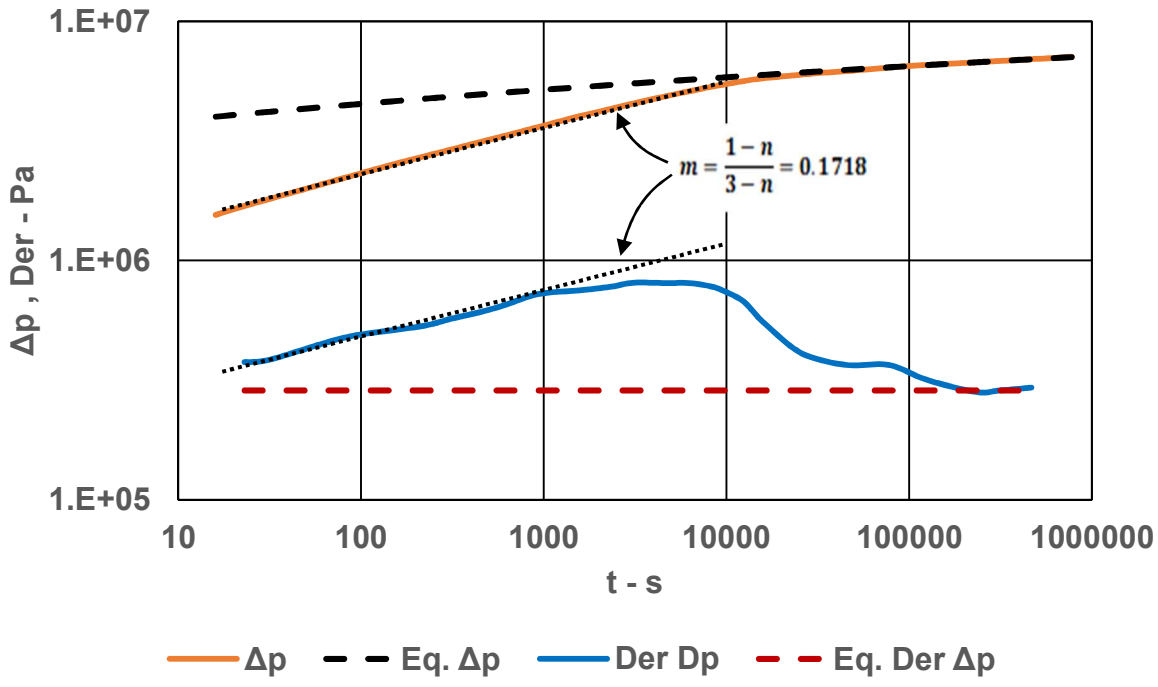

Figure 6.2. Diagnostic plot for a power-law type fluid, n = 0.6 (Lund and Ikoku, 1981).

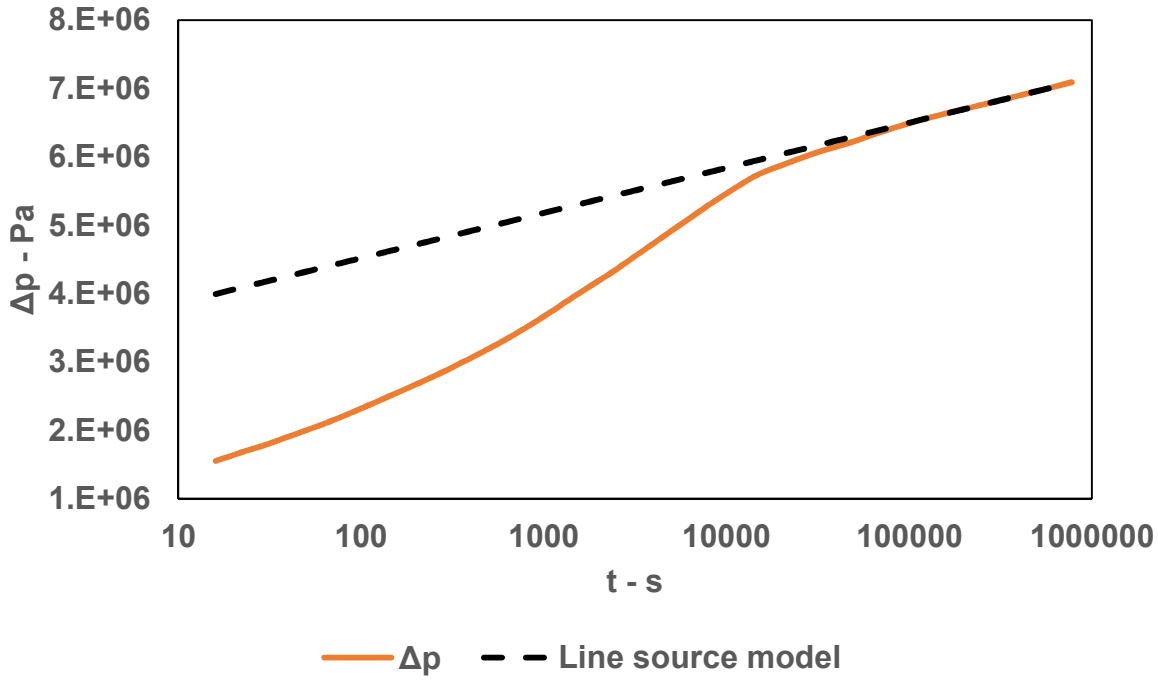

Figure 6.3. Semi-log plot for a power-law type fluid, n = 0.6 (Lund and Ikoku, 1981).

6.2.2 Dilatant type fluid

The Lund-Ikoku model was used to simulate the behavior of a Dilatant type fluid. The properties for this system are reported in **Table 6. 2**, considering for the simulation a constant radius of influence of $r_{D_{NN}} = 300$ and no wellbore storage effects. **Figures 6.4 and 6.5** present the diagnostic and semi-log plots for the analyzed problem.

Table 6. 2. Obtained values of the pseudo-skin factor for power-law type fluids.

r_w, m	0.1	k, md	100
h, m	5	$q, m^3/s$	5.5204×10^{-4}
$\phi, fraction$	0.2	c_t, Pa^{-1}	1×10^{-9}
r_{NN}, m	40	$H, N\cdot s^n/m^2$	0.02
n	1.1	$\mu_n, Pa\cdot s$	0.02

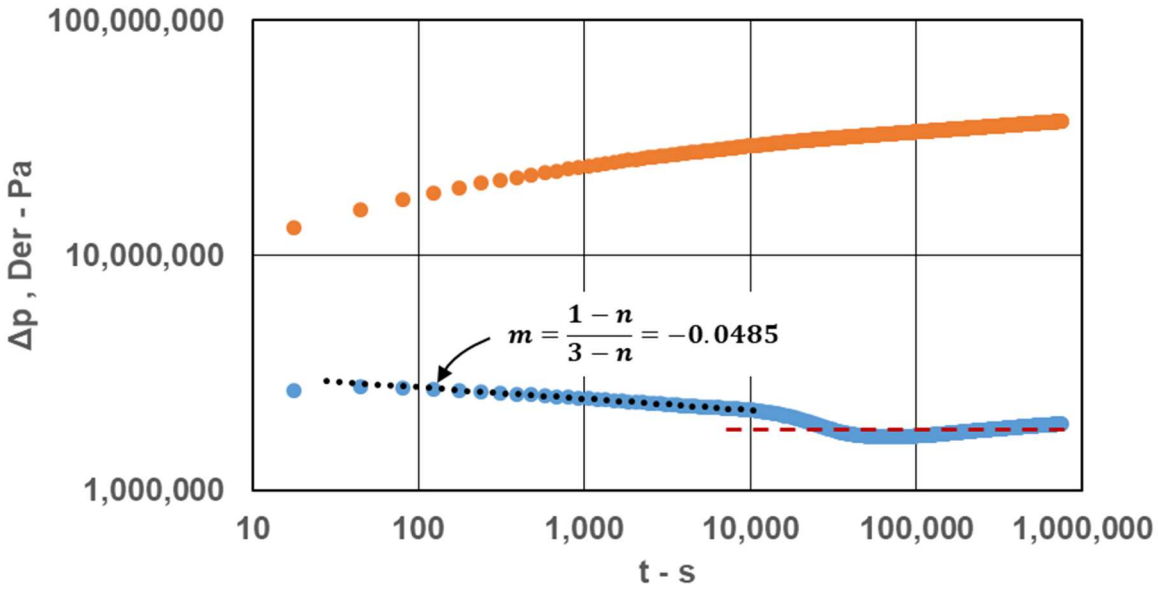

Figure 6.4. Diagnostic plot for a power-law type fluid, n = 1.1.

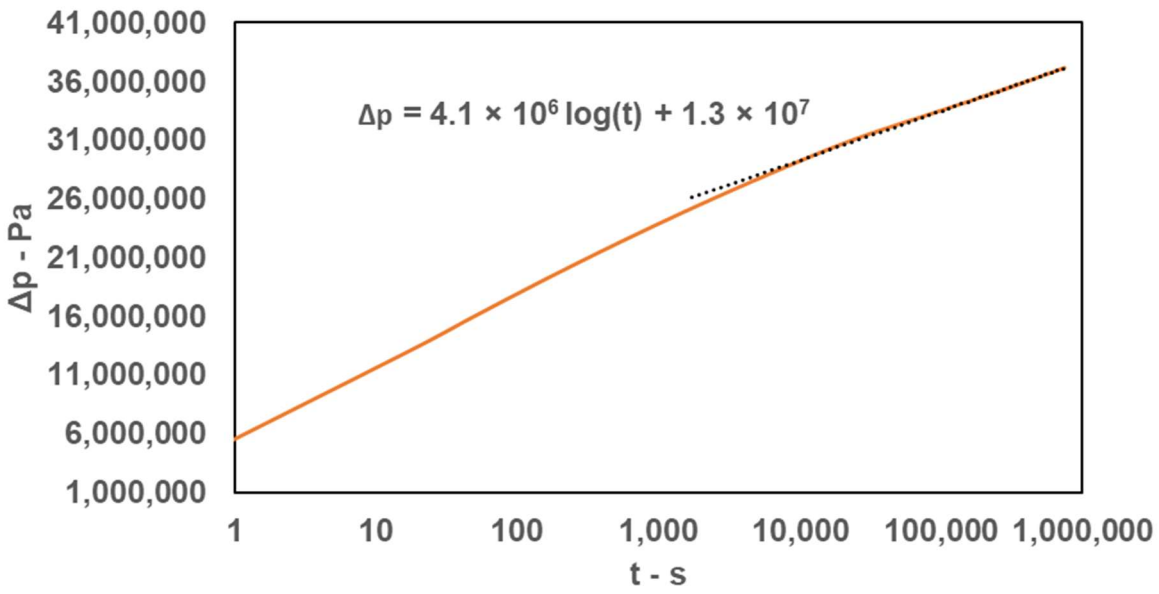

Figure 6.5. Semi-log plot for a power-law type fluid, n = 1.1.

In the diagnostic plot, both the power-law and the Newtonian slopes were analyzed from the derivative curve. From the first part of this graph, a slope of -0.0485 was observed, which interpreted with Ikoku-Ramey method leads to a value of $n = 1.093$, corresponding with the input value of $n = 1.1$; and at the Newtonian stabilized segment a value of 1852896 Pa was observed, from which a permeability of 96 md was interpreted. As well, a slope of 4.1 × 10^6 $Pa\ /\ cycle$ and a value of Δp_w at 1 second of 1.3 × 10^7 Pa were obtained from the late straight-line in the semi-log plot, for which a permeability of 100 md and a total skin factor of 3.46 were determined.

Finally, when computing the skin factor with Eq. 4.21 (μ_{eff} = 6.02 × 10^{-6} $N \cdot s^{0.6} / m^{1.6}$, Eq. 2.6) a value of 3.55 was obtained, which is practically the same interpreted.

6.2 Bingham plastic fluids

The models for the flow of a Bingham plastic fluid were validated with a numerical simulator, which formulation is included in **Appendix C**. The cases for G_D = 0, 0.01, 0.1

and 1.0 are presented in **Figs. 6.6 to 6.8**, respectively; also, for $G_D = 0$, Theis solution was included. Results for the dimensionless downhole pressure and its logarithmic time derivative –obtained with the numerical simulator– are presented in **Fig. 6.9** for values of G_D = 0, 0.001, 0.01, 0.1, 1.0 and 2.0 in a log-log plot for a finite radial system of r_{eD} =200.

It is seen from Figs. 6.6 to 6.8 that the proposed analytical solutions and the Wu's approximation correctly fit the observed behavior of the numerical solution. However, the use of Eq. 5.17 is bounded for values of G_D lower than 1. Also, as expected, from Fig. 6.7 it is concluded that a more efficient use of the pressure energy is achieved when G_D has small values. Indeed, large values of G_D may provoke operational problems in a well, such as production interruption or intermittent production profiles for not overcoming the condition of the minimum flow gradient in the reservoir[23, 24]. Yet, as this parameter inversely depends on the production-rate: the higher the flow velocity gets in the porous media, the lower the influence of G_D is; consequently a small p_{wf} and the use of an artificial lift system may improve conditions of Newtonian flow near the well.

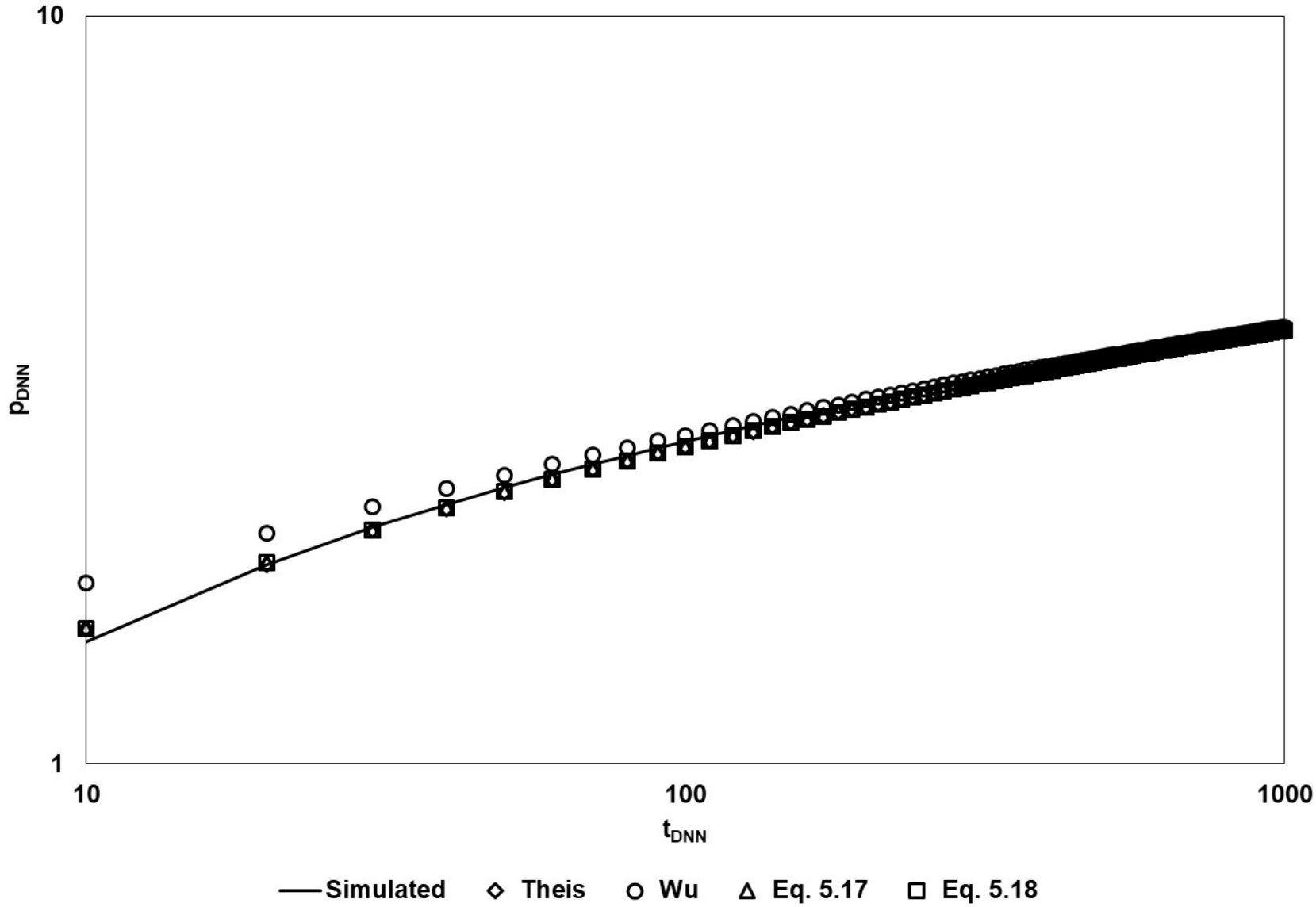

Figure 6.6. Comparison between flow-solutions for a Newtonian fluid ($G_D = 0$) in a logarithmic plot.

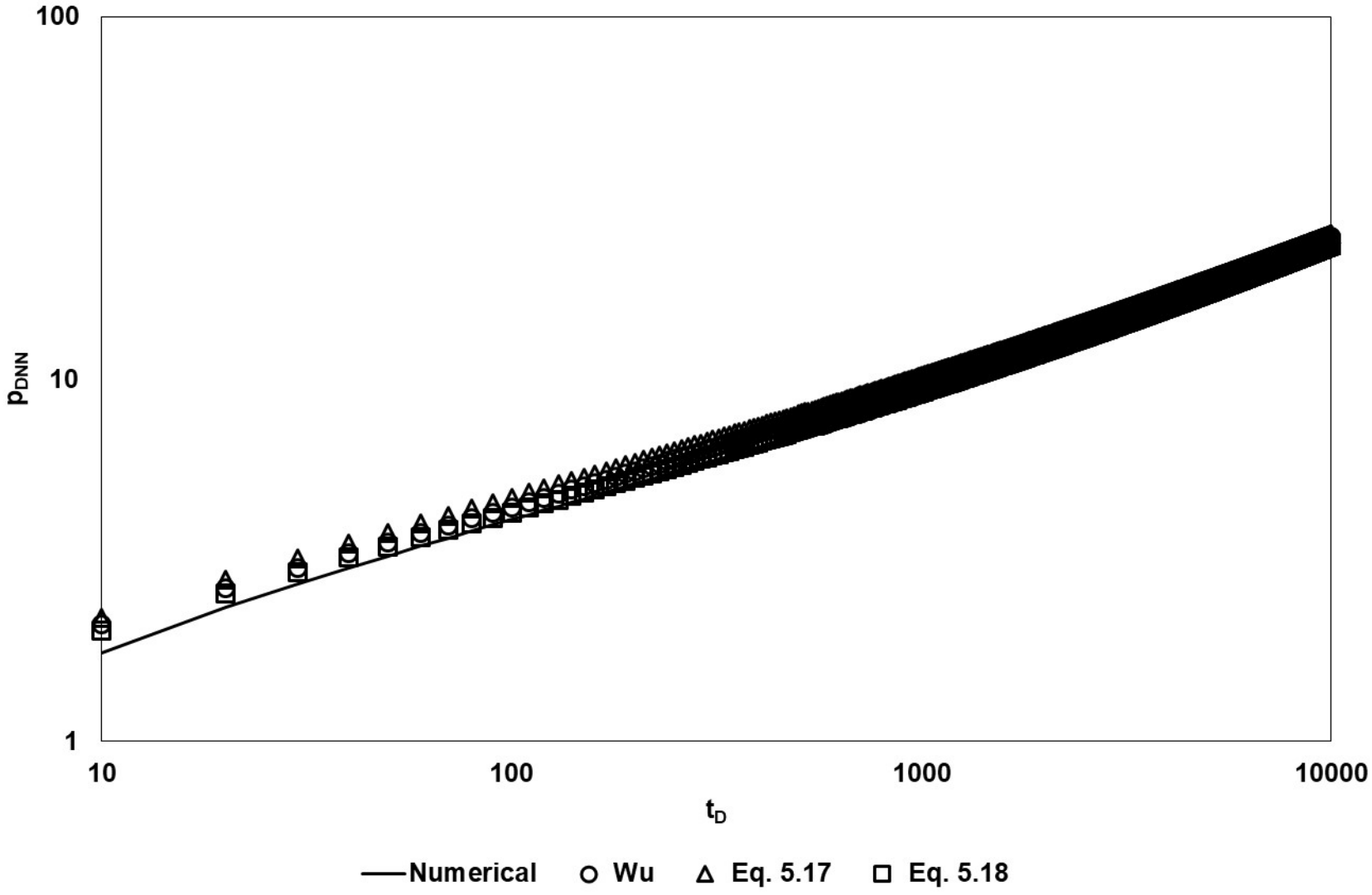

Figure 6.7. Comparison between flow-solutions for a Bingham plastic fluid of $G_D = 0.1$ in a logarithmic plot.

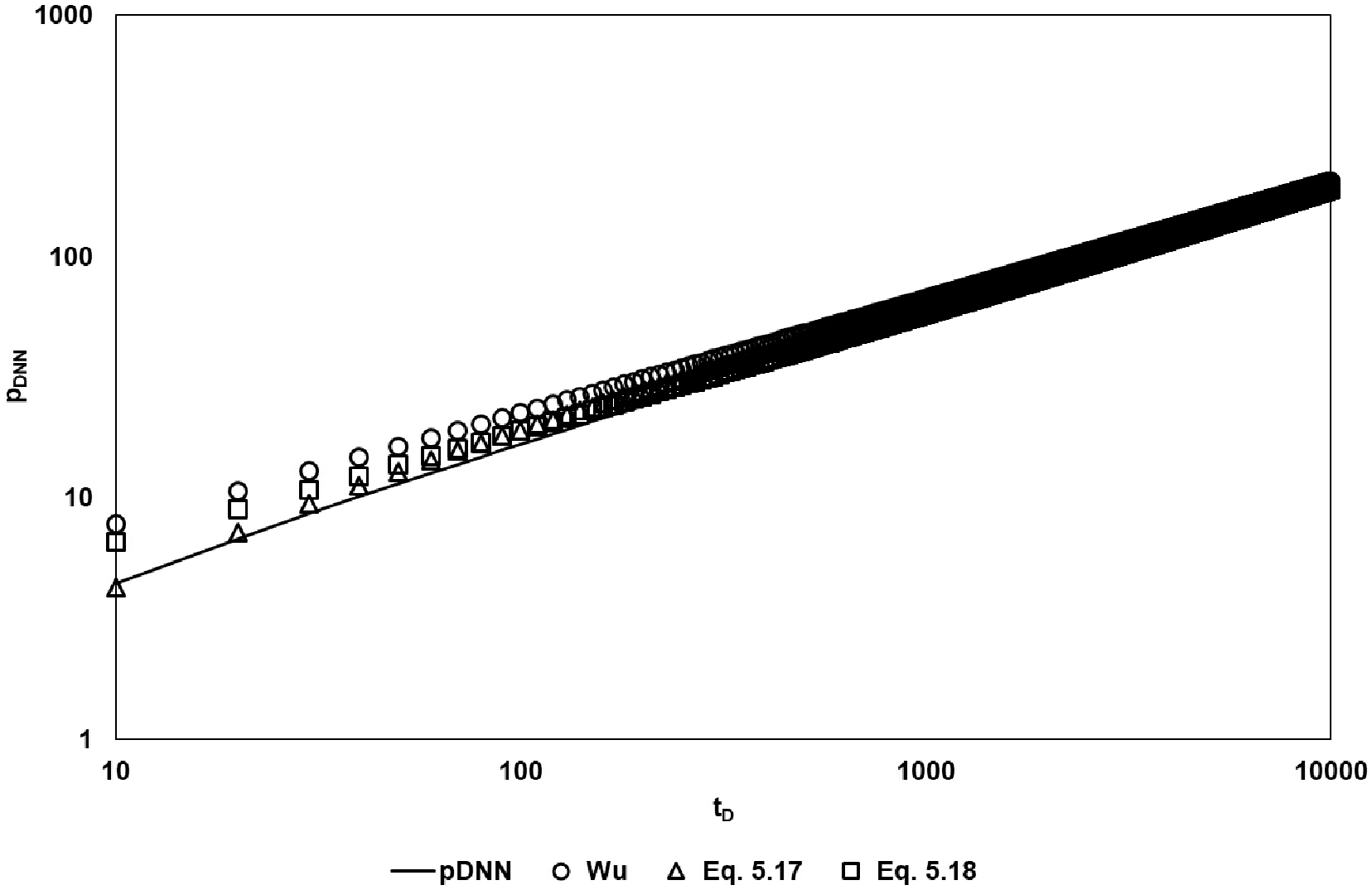

Figure 6.8. Comparison between flow-solutions for a Bingham plastic fluid of $G_D = 1$ in a logarithmic plot.

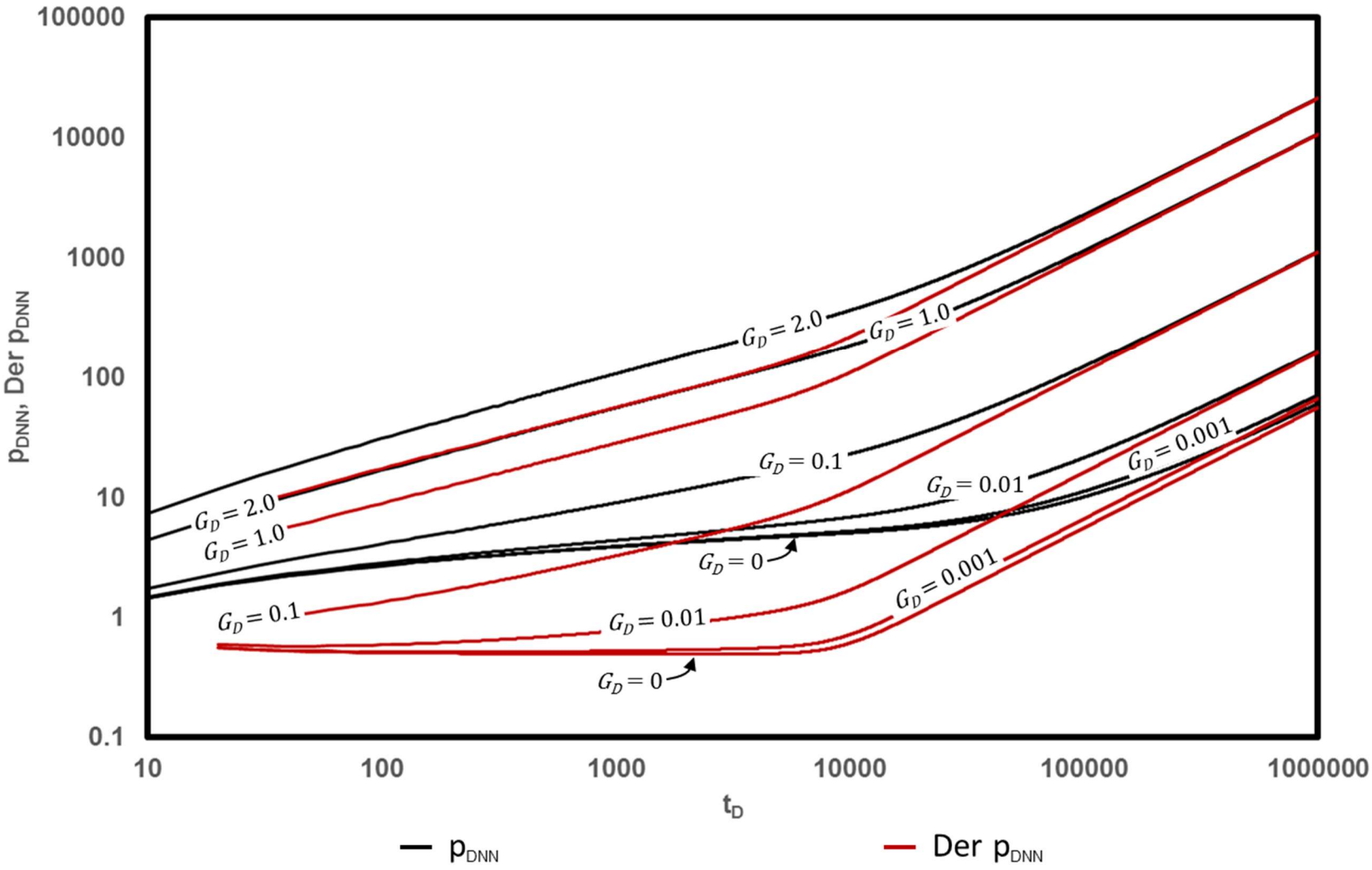

Figure 6.9. Comparison between the values of the dimensionless pressure drop for a Newtonian and a Non-Newtonian Bingham plastic fluid in a finite radial reservoir of $r_{eD} = 200$ (cases for G_D = 0.001, 0.01, 0.1, 1 and 2).

Conclusions

A study was made over the rheological aspects of heavy and extra-heavy oil, for which the following conclusions are made:

1. Non-Newtonian power-law and Bingham plastic cases were studied, specifically the models of Ikoku and Wu, respectively. For the Bingham plastic case, dimensionless groups were developed to generalize the analysis.

2. Considering the existence of viscoelastic effects in a fluid, a model to represent the power-law effects with a pseudo-skin factor was developed. It was seen that the required pressure energy for its transport is greater for a pseudo-plastic fluid than for a dilatant.

3. Two new analytical solutions were obtained for the case of radial flow of a Bingham plastic fluid produced at constant rate. Its performance was compared with Wu's integral solution, obtaining a better match when compared with the simulated values.

4. An approximation was presented to calculate the value of the penetration distance of the wellbore stimulus into the reservoir.

5. With the developed simulator it was seen that, for Bingham plastic fluids, the value of G_D nor affect the value of time at which the boundaries are affected by a wellbore stimulus, neither the behavior of the pseudo-steady state period. However, it considerably affects the pressure response by imposing a restriction to the flow.

Recomendations

During this research, several aspects that were neglected may require more consideration and the results of our research should be applied in practice. Hence, some recommendations will be list as follows:

1. In the case of power-law type fluids, it is expected that the value of n must be pressure dependent, and more detailed studies can be done to obtain relations between this parameters for the different kinds of oils. Inconsequence, the radius of influence for the power-law behavior must be a time dependent value.

2. The validation of the developed model to represent the non-Newtonian pseudo-skin factor for power-law type fluids can be extended for more cases.

3. During the literature review it was found that, besides TOUGH, commercial software do not consider the use of non-Newtonian flow models. Hence, the development of studies should be extended for the correct study of geofluid systems.

References

1. Guzman, R. (2015). Trends and Challenges in the Heavy Crude Oil Market. Presentation, 4th Heavy Oil Working Group, Bogota.

2. Banerjee, D. (2012). Oil sands, heavy oil & bitumen. Tulsa, Okla.: PennWell Corp.

3. Prowse, D., & Ivory, J. (1983). Some physical properties of bitumen and oil sand. Edmonton: Alberta Research Council, Oil Sands Research Dept.

4. Wallace, D., & Starr, J. (1988). Characterization of oil sand resources. Edmonton: Alberta Oil Sands Technology and Research Authority.

5. Argillier, J.-F., Coustet, C., & Henaut, I. (2002, January 1). Heavy Oil Rheology as a Function of Asphaltene and Resin Content and Temperature. Society of Petroleum Engineers. doi:10.2118/79496-MS.

6. Huang, W. S. B., Marcum, B. E., Chase, M. R., & Yu, C. L. (1997, January 1). Cold Production of Heavy Oil from Horizontal Wells in the Frog Lake Field. Society of Petroleum Engineers. doi:10.2118/37545-MS.

7. De Mirabal, M., Gordillo, R., Fuenmayor, M., Rojas, G., Rodriguez, H., & Sanchez, R. (1996, January 1). Integrated Study for the Characterization and Development of the MFB-53 Reservoir, North Hamaca-Orinoco Belt, Venezuela. Society of Petroleum Engineers. doi:10.2118/36095-MS.

8. De Mirabal, M., Rodriguez, H., & Gordillo, R. (1997, January 1). Production Improvement Strategy For Foamy Hamaca Crude Oil: A Field Case. Society of Petroleum Engineers. doi:10.2118/37544-MS.

9. Maini, B. (1998, April 1). Is It Futile to Measure Relative Permeability For Heavy Oil Reservoirs? Petroleum Society of Canada. doi:10.2118/98-04-06.

10. Maini, B. B. (2001, October 1). Foamy-Oil Flow. Society of Petroleum Engineers. doi:10.2118/68885-JPT.

11. Rojas, G., Barrios, T., Scudeiro, B., & Ruiz, J. (2017). Rheological Behaviour of Extra-Heavy Crude Oils from the Orinoco Oil Belt. Oil Sands, 1, 284-302.

12. Prowse, D., & Ivory, J. (1983). Some physical properties of bitumen and oil sand. Edmonton: Alberta Research Council, Oil Sands Research Dept.

13. Poon, D., & Kisman, K. (1992, July 1). Non-Newtonian Effects On The Primary Production Of Heavy Oil Reservoirs. Petroleum Society of Canada. doi:10.2118/92-07-06.

14. Smith, G. E. (1988, May 1). Fluid Flow and Sand Production in Heavy-Oil Reservoirs Under Solution-Gas Drive. Society of Petroleum Engineers. doi:10.2118/15094-PA.

15. Maini, B. B., Sarma, H. K., & George, A. E. (1993, September 1). Significance of Foamy-oil Behaviour In Primary Production of Heavy Oils. Petroleum Society of Canada. doi:10.2118/93-09-07

16. D.S. George, O. Hayat, and A.R. Kovscek. A Microvisual Study of Solution-GasDrive Mechanisms in Viscous Oils. Journal of Petroleum Science & Engineering, 46(1-2):101–119, 2004.

17. Dusseault, M. B. (1993, January 1). Stress Changes in Thermal Operations. Society of Petroleum Engineers. doi:10.2118/25809-MS.

18. Wang, Y., & Chen, C. C. (2001, October 1). Enhanced Oil Production Owing to Sand Flow in Conventional and Heavy-Oil Reservoirs. Society of Petroleum Engineers. doi:10.2118/73827-PA.

19. Wang, Y., & Chen, C. Z. (2004, April 1). Simulating Cold Heavy Oil Production With Sand by Reservoir-Wormhole Model. Petroleum Society of Canada. doi:10.2118/04-04-03.

20. Miller, K. A., & Erno, B. P. (1995, January 1). Use And Misuse of Heavy Oil And Bitumen Viscosity Data. Petroleum Society of Canada. doi:10.2118/95-93.

21. Cruz, B. (2012). *Determinación del comportamiento reológico de los aceites extrapesados a condiciones de yacimiento* (Undergraduate). Universidad Nacional Autónoma de México.

22. Wu, Y.-S., Pruess, K., & Witherspoon, P. A. (1992, August 1). Flow and Displacement of Bingham Non-Newtonian Fluids in Porous Media. Society of Petroleum Engineers. doi:10.2118/20051-PA.

23. Wu, Y-S. "Theoretical Studies of Non-Newtonian and Newtonian Fluid Flow Through Porous Media," PhD dissertation, U. of California, Berkeley (1990).

24. Mirzadjanzade, A. K., Akhmedov, Z. M., Gurbanov, R. S., Amirov, A. D., Barenblatt, G. I., Entov, V. M., & Zaitsev, Y. V. (1971, January 1). On the Special Features of Oil and Gas Field Development Due to Effects of Initial Pressure Gradients. World Petroleum Congress.

25. Hubbert, M.K. 1956. Darcy's Law and the Field Equations of the Flow of Underground Fluids. In: Society of Petroleum Engineers.

26. Sochi, T. (2010). Non-Newtonian flow in porous media. *Polymer*, *51*(22), 5007-5023. http://dx.doi.org/10.1016/j.polymer.2010.07.047.

27. Ikoku, C. U., & Ramey, H. J. (1979, June 1). Transient Flow of Non-Newtonian Power-Law Fluids in Porous Media. Society of Petroleum Engineers. doi:10.2118/7139-PA.

28. Omosebi, O. A., & Akabogu, A. K. (2017, April 23). Application of the Galerkin's Finite Element Method to the Flow of Power-Law Non-Newtonian Fluids through Porous Media. Society of Petroleum Engineers. doi:10.2118/185689-MS.

29. Dong, X., Liu, H., Wang, Q., Pang, J., Wang, C. (2013) Non-Newtonian flow characterization of heavy crude oil in porous media. Journal of Petroleum Exploration and Production Technology, 3:43. https://doi.org/10.1007/s13202-012-0043-9.

30. Yun, M., Yu, B., Lu, J., Zheng, W. (2010) Fractal analysis of Herschel–Bulkley fluid flow in porous media. International Journal of Heat and Mass Transfer. https://doi.org/10.1016/j.ijheatmasstransfer.2010.04.020.

31. Bondor, P. L., Hirasaki, G. J., & Tham, M. J. (1972, October 1). Mathematical Simulation of Polymer Flooding in Complex Reservoirs. Society of Petroleum Engineers. doi:10.2118/3524-PA.

32. Kraus, W. P., McCaffrey, W. J., & Boyd, G. W. (1993, January 1). Pseudo-Bubble Point Model For Foamy Oils. Petroleum Society of Canada. doi:10.2118/93-45.

33. Claridge, E. L., and Prats, M.: 1995, A proposed model and mechanism for anomalous foamy heavy oil behavior, SPE 29243.

34. Lillico, D., Babchin, A., Jossy, W., Sawatzky, R., & Yuan, J. (2001). Gas bubble nucleation kinetics in a live heavy oil. *Colloids And Surfaces A: Physicochemical And Engineering Aspects*, *192*(1-3), 25-38.

35. Sahni, A., Gadelle, F., Kumar, M., Tomutsa, L., & Kovscek, A. R. (2004, June 1). Experiments and Analysis of Heavy-Oil Solution-Gas Drive. Society of Petroleum Engineers. doi:10.2118/88442-PA.

36. Cassani, F., Ortega, P., Davila, A., Rodriguez, W., & Seranno, J. (1992, January 1). Evaluation of Foam Inhibitors at the Jusepin Oil/Gas Separation Plant, El Furrial Field, Eastern Venezuela. Society of Petroleum Engineers. doi:10.2118/23681-MS.

37. Adil, I., & Maini, B. B. (2005, January 1). Role of Asphaltene in Foamy-Oil Flow. Society of Petroleum Engineers. doi:10.2118/94786-MS.

38. Sheng, J. J., Maini, B. B., Hayes, R. E., & Tortike, W. S. (1997, April 1). Experimental Study of Foamy Oil Stability. Petroleum Society of Canada. doi:10.2118/97-04-02.

39. Ostos, A., & Maini, B. (2004, January 1). Capillary Number in Heavy Oil Solution Gas Drive and Its Relationship with Gas-Oil Relative Permeability Curves. Society of Petroleum Engineers. doi:10.2118/89430-MS.

40. Maini, B. (1996, June 1). Foamy Oil Flow In Heavy Oil Production. Petroleum Society of Canada. doi:10.2118/96-06-01.

41. Maini, B. B. (2003, January 1). Effect of Depletion Rate on Performance of Solution-Gas Drive in Heavy Oil Systems. Society of Petroleum Engineers. doi:10.2118/81114-MS.

42. Sheng, J. J., Maini, B. B., Hayes, R. E., & Tortike, W. S. (1999, April 1). A Non-equilibrium Model to Calculate Foamy Oil Properties. Petroleum Society of Canada. doi:10.2118/99-04-04.

43. Alshmakhy, A., & Maini, B. B. (2012, January 1). Foamy-Oil-Viscosity Measurement. Society of Petroleum Engineers. doi:10.2118/136665-PA.

44. Dusseault, M. B., Geilikman, M. B., & Roggensack, W. D. (1995, January 1). Practical Requirements for Sand Production Implementation in Heavy Oil Applications. Society of Petroleum Engineers. doi:10.2118/30250-MS.

45. Yalamas, T., Nauroy, J. F., Bemer, E., Dormieux, L., & Garnier, D. (2004, January 1). Sand Erosion in Cold Heavy-Oil Production. Society of Petroleum Engineers. doi:10.2118/86949-MS.

46. Kumar, R., & Pooladi-Darvish, M. O. (2001, March 1). Effect of Viscosity and Diffusion Coefficient on the Kinetics of Bubble Growth in Solution-Gas Drive in Heavy Oil. Petroleum Society of Canada. doi:10.2118/01-03-02.

47. Wang, Y., Chen, C. C., & Dusseault, M. B. (2001, January 1). An Integrated Reservoir Model for Sand Production and Foamy Oil Flow During Cold Heavy Oil Production. Society of Petroleum Engineers. doi:10.2118/69714-MS.

48. Wang, Y., & Chen, C. Z. (2004, April 1). Simulating Cold Heavy Oil Production With Sand by Reservoir-Wormhole Model. Petroleum Society of Canada. doi:10.2118/04-04-03.

49. Wan, R. G., & Liu, Y. (2005, January 1). Finite Element Modelling of Sand Production Under Foamy Oil Flow in Heavy Oil Reservoirs. Petroleum Society of Canada. doi:10.2118/2005-214.

50. Dusseault, M. B., & Santarelli, F. J. (1989, January 1). A Conceptual Model For Massive Solids Production In Poorly-consolidated Sandstones. International Society for Rock Mechanics.

51. Loughead, D. J., and Saltuklaroglu, M. 1992. Lloydminster Heavy OilProduction: Why so Unusual? Oral presentation, given at the Ninth Annual HeavyOil and Oil Sands Technology Symposium, Calgary, Alberta, Canada, 11 March.

52. Ikoku, C. U., & Ramey, H. J. (1978, January 1). Numerical Solution Of The Nonlinear Non-Newtonian Partial Differential Equation. Society of Petroleum Engineers. doi:NA.

53. Ikoku, C. U., & Ramey, H. J. (1980, February 1). Wellbore Storage and Skin Effects During the Transient Flow of Non-Newtonian Power-Law Fluids in Porous Media. Society of Petroleum Engineers. doi:10.2118/7449-PA.

54. Ikoku, C. U., & Ramey, H. J. (1978, January 1). Flow Of Foam In Porous Media. Society of Petroleum Engineers. doi:NA.

55. Lund, O., & Ikoku, C. U. (1981, April 1). Pressure Transient Behavior of Non-Newtonian/Newtonian Fluid Composite Reservoirs. Society of Petroleum Engineers. doi:10.2118/9401-PA.

56. Vongvuthipornchai, S., & Raghavan, R. (1987, December 1). Well Test Analysis of Data Dominated by Storage and Skin: Non-Newtonian Power-Law Fluids. Society of Petroleum Engineers. doi:10.2118/14454-PA.

57. Wu, X. (1990, January 1). Study of Oil/Water Movement in Heterogeneous High-Viscosity Zones. Society of Petroleum Engineers.

Appendix A

Development of Eqs. 5. 17 and 5. 18: Production of a Bingham-plastic fluid at constant rate in an infinite reservoir

$$\frac{1}{r}\frac{\partial}{\partial r}\left[r\left(\frac{\partial p}{\partial r}-G\right)\right]=\frac{\mu_B c_t \phi}{k}\frac{\partial p}{\partial t}\ , \quad \text{..... A. 1}$$

$$p(r,t=0)=p_i\ , \quad \text{..... A. 2}$$

$$q(r_w,t>0)=q_w\ , \quad \text{..... A. 3}$$

$$p(r\to\infty,t>0)=p_i\ . \quad \text{..... A. 4}$$

A.1 Development of Eq. 5. 17

The following expression for an effective pressure is proposed:

$$\psi=p-Gr\ , \quad \text{..... A. 5}$$

hence

$$\frac{\partial \psi}{\partial r}=\frac{\partial p}{\partial r}-G\ , \quad \text{..... A. 6}$$

and the following variable change is made on Eq. A. 1

$$\frac{1}{r}\frac{\partial}{\partial r}\left[r\frac{\partial \psi}{\partial r}\right]=\frac{\mu_B c_t \phi}{k}\frac{\partial p}{\partial t}\frac{\partial \psi}{\partial \psi}=\frac{\mu_B c_t \phi}{k}\frac{\partial \psi}{\partial t}\frac{\partial p}{\partial \psi}\ ,$$

where

$$\frac{\partial p}{\partial \psi}=1+G\frac{\partial r}{\partial \psi}=1+\frac{G}{\partial \psi/\partial r}\ . \quad \text{..... A. 7}$$

Now, as the flow-rate across a reservoir section is

$$q_r=-\frac{kA}{\mu_B}\frac{\partial \psi}{\partial r}\ ,$$

it can be obtained that

$$\frac{\partial \psi}{\partial r}=-\frac{q_r \mu_B}{kA}\ ,$$

and Eq. A. 7 results in:

$$\frac{\partial p}{\partial \psi}=1-\frac{kAG}{\mu_B}q_r^{-1}=1-\chi q_r^{-1}\ . \quad \text{..... A. 8}$$

Strictly, q_r changes over the drainage area of a well. However, as flow can only exist across the radius of investigation if the pressure gradient is more than G, it is considered that the transient flow can be analyzed as a series of steady periods, for which $q_r = qB$ and the following factor is defined:

$$\xi_r=\frac{\partial p}{\partial \psi}=1-G_D\ , \quad \text{..... A. 9}$$

and Eq. 1 is written as:

$$\frac{1}{r}\frac{\partial}{\partial r}\left[r\frac{\partial \psi}{\partial r}\right]=\frac{\mu_B c_t \phi}{k}\xi_r\frac{\partial \psi}{\partial t}\ . \quad \text{..... A. 10}$$

Now, based in the statement presented in Section 5.1, it is proposed that the influence of the threshold gradient can be modeled by adding the initial pressure drop exerted by the well to induce flow and the pressure drop due to the transport of the minimum gradient condition across the reservoir as follows:

$$p(r,t) = p_i - \{\psi(r,t) + G[r_w + \delta(t)]\} \ . \quad \text{..... A. 11}$$

Here, considering the dimensionless group presented in Section 5.2, the following variables are defined:

$$\psi_{D_{NN}} = \frac{2\pi kh}{qB\mu_B}(p_i - \psi) \ , \quad \text{..... A. 12}$$

$$r_D = r/r_w \ , \quad \text{..... A. 13}$$

$$t^*_{D_{NN}} = \frac{\eta_B}{r_w^2}\xi_r t \ , \quad \text{..... A. 14}$$

$$G_D = \frac{2\pi khr_w}{qB\mu_B}G \ , \quad \text{..... A. 15}$$

and the flow problem is rewritten as:

$$\frac{\partial^2\psi_{D_{NN}}}{\partial r_D^2} + \frac{1}{r_D}\frac{\partial\psi_{D_{NN}}}{\partial r_D} = \frac{\partial\psi_{D_{NN}}}{\partial t^*_{D_{NN}}} \ , \quad \text{..... A. 16}$$

$$\psi_{D_{NN}}\left(r_D, t^*_{D_{NN}} = 0\right) = 0 \ , \quad \text{..... A. 17}$$

$$r_D\frac{\partial\psi_{D_{NN}}}{\partial r_D}\left(1, t^*_{D_{NN}} > 0\right) = -1 \ , \quad \text{..... A. 18}$$

$$\psi_{D_{NN}}\left(r \to \infty, t^*_{D_{NN}} > 0\right) = 0 \ . \quad \text{..... A. 19}$$

To solve this problem, the Laplace transform method was used, for which it is defined

$$\bar{\Psi}_D = \int_0^{\infty} \psi_{D_{NN}} e^{-Z t_D^*} dt_{D_{NN}}^* \ , \quad \text{..... A. 20}$$

and the flow problem is now expressed as

$$\frac{\partial^2 \bar{\Psi}_D}{\partial r_D^2} + \frac{1}{r_D}\frac{\partial \bar{\Psi}_D}{\partial r_D} = Z\bar{\Psi}_D - \psi_{D_{NN}}\left(t_{D_{NN}}^* = 0\right) \ , \quad \text{..... A. 21}$$

$$r_D \frac{\partial \bar{\Psi}_D}{\partial r_D}(r_D = 1) = -\frac{1}{Z} \ , \quad \text{..... A. 22}$$

$$\bar{\Psi}_D(r_D \to \infty) = 0 \ . \quad \text{..... A. 23}$$

The solution of Eq. A. 21 is

$$\bar{\Psi}_D = \alpha_1 K_0\left(\xi_r \sqrt{Z} r_D\right) + \alpha_2 I_0\left(\xi_r \sqrt{Z} r_D\right) \ , \quad \text{..... A. 24}$$

which evaluated in the boundary conditions leads to:

$$\alpha_1 = \frac{K_1\left(\sqrt{Z} r_D\right)}{Z^{3/2}} \ , \quad \text{..... A. 25}$$

$$\alpha_2 = 0 \ . \quad \text{..... A. 26}$$

Finally, substituting α_1 and α_2 in Eq. A. 24 results in:

$$\bar{\Psi}_D = \frac{K_1\left(\sqrt{Z} r_D\right) K_0\left(\xi_r \sqrt{Z} r_D\right)}{Z^{3/2}} \ , \quad \text{..... A. 27}$$

which when inverted is expressed as:

$$\psi_D\left(r_D, t_{D_{NN}}\right) = -0.5\, \mathrm{E_i}\left(-\frac{4 r_D^2}{t_{D_{NN}}}\right) + 0.5 \ln|\xi| \ , \quad \text{..... A. 28}$$

and using the dimensionless form of the Eq. A. 11:

$$p_{D_{NN}}(r_D, t_{D_{NN}}) = -0.5\,\mathrm{E_i}\left(-\frac{4r_D^2}{t_{D_{NN}}}\right) + 0.5\ln|\xi| + G_D\left[1 + \delta_D\left(t_{D_{NN}}\right)\right] , \quad \text{..... A. 29}$$

where $p_{D_{NN}}$ is defined in Eq. 5. 6.

A.2 Development of Eq. 5. 18

Recalling the slightly fluid approach presented in Section 5.3:

$$\frac{\partial^2 p_{D_{NN}}}{\partial r_D^2} + \frac{1}{r_D}\frac{\partial p_{D_{NN}}}{\partial r_D} + \frac{G_D}{r_D} = \frac{\partial p_{D_{NN}}}{\partial t_{D_{NN}}} , \quad \text{..... A. 30}$$

$$p_{D_{NN}}(r_D, 0) = 0 , \quad \text{..... A. 31}$$

$$\left(r_D \frac{\partial p_{D_{NN}}}{\partial r_D}\right)_{r_D=1} = -1 - G_D \qquad t_{D_{NN}} > 0 , \quad \text{..... A. 32}$$

$$p_{D_{NN}}(r_D \to \infty) = 0 \qquad t_{D_{NN}} > 0 . \quad \text{..... A. 33}$$

And deffining the Laplace transform as

$$\overline{\mathrm{P}}_D = \int_0^\infty p_{D_{NN}} e^{-Z t_{D_{NN}}} dt_{D_{NN}} , \quad \text{..... A. 34}$$

when transforming the initial problem, it follows that

$$\frac{d^2\overline{\mathrm{P}}_D}{dr_D^2} + \frac{1}{r_D}\frac{d\overline{\mathrm{P}}_D}{dr_D} + \frac{G_D}{Z r_D} = Z\overline{\mathrm{P}}_D - p_{D_{NN}}\left(t^*_{D_{NN}} = 0\right) , \quad \text{..... A. 35}$$

$$r_D \frac{d\overline{\mathrm{P}}_D}{dr_D}(r_D = 1) = -\frac{1}{Z} + \frac{G_D}{Z} \ , \quad \text{..... A. 36}$$

$$\overline{\mathrm{P}}_D(r_D \to \infty) = 0 \ . \quad \text{..... A. 37}$$

Now, defining the Boltzmann variable as $X = \sqrt{Z} r_D$, Eq. A.30 can be expressed as

$$X^2 \frac{d^2\overline{\mathrm{P}}_D}{dX^2} + X \frac{d\overline{\mathrm{P}}_D}{dX} + \frac{r_D}{Z} G_D - X^2 \overline{\mathrm{P}}_D = 0 \ . \quad \text{..... A. 38}$$

As seen, Eq. A. 30 is a non-homogenous form of the modified Bessel equation, which its homogenous associated solution ($\bar{P}_{D_H}$) is given by:

$$\bar{P}_{D_H} = \alpha_1 I_0(X) + \alpha_2 K_0(X) \ , \quad \text{..... A. 39}$$

and its general solution is obtained by including both, the particular ($\overline{\mathrm{P}}_{D_p}$) and associated solutions as:

$$\overline{\mathrm{P}}_D = \overline{\mathrm{P}}_{D_p} + \bar{P}_{D_H} = \overline{\mathrm{P}}_{D_p} + \alpha_1 I_0(X) + \alpha_2 K_0(X) \ , \quad \text{..... A. 40}$$

which solution can be known by mean of the variation of parameters method. For it, it is proposed that particular solution fits to a polynomial of the form of:

$$\overline{\mathrm{P}}_{D_p} = \beta_1(X) I_0(X) + \beta_2(X) K_0(X) \ , \quad \text{..... A. 41}$$

where $\beta_1(X)$ and $\beta_2(X)$ are unknown variable coefficients, which satisfy the following restriction

$$\beta_1'(X) I_0(X) + \beta_2'(X) K_0(X) = 0 \ , \quad \text{..... A. 42}$$

where $\beta_1'(X)$ and $\beta_2'(X)$ are the first derivatives of the coefficients.

Now, to solve Eq. A. 41, the first and second derivatives are obtained, considering Eq. A. 42, as:

$$\overline{\mathrm{P}}_{D_p}{}' = \beta_1(X)I_0'(X) + \beta_2(X)K_0'(X) \ ,$$

$$\overline{\mathrm{P}}_{D_p}{}'' = \beta_1'(X)I_0'(X) + \beta_1(X)I_0''(X) + \beta_2'(X)K_0'(X) + \beta_2(X)K_0''(X) \ .$$

Both derivatives are substituted in Eq. A. 38

$$X^2[\beta_1'(X)I_0'(X) + \beta_1(X)I_0''(X) + \beta_2'(X)K_0'(X) + \beta_2(X)K_0''(X)] + X[\beta_1(X)I_0'(X) + \beta_2(X)K_0'(X)] - X^2[\beta_1(X)I_0(X) + \beta_2(X)K_0(X)] = -\frac{r_D}{Z}G_D \ ,$$

or rearranging:

$$X^2[\beta_1'(X)I_0'(X) + \beta_2'(X)K_0'(X)] + \beta_1(X)[X^2I_0''(X) + XI_0'(X) - X^2I_0(X)] + \beta_2(X)[X^2K_0''(X) + XK_0'(X) - X^2K_0(X)] = -\frac{r_D}{Z}G_D \ ,$$

Since both $I_0(X)$ and $K_0(X)$ are solutions to the homogenous problem, the second and third terms are zero. Acknowledging this and rearranging, the resulting expression is:

$$X^2[\beta_1'(X)I_0'(X) + \beta_2'(X)K_0'(X)] = -\frac{r_D}{Z}G_D \ ,$$

or

$$\beta_1'(X)I_0'(X) + \beta_2'(X)K_0'(X) = \lambda(Z) = -\frac{G_D}{Z^{3/2}X} \ . \quad \text{..... A. 43}$$

Eqs. A. 42 and A. 43 can be algebraicly treated so:

$$\beta_1'(X) = -\frac{\beta_2'(X)K_0(X)}{I_0(X)} \ ,$$

$$-\frac{\beta_2'(X)}{I_0(X)}[I_1(X)K_0(X) + K_1(X)I_0(X)] = -\frac{G_D}{Z^2r_D} \ ,$$

where the Wronskian of the modified Bessel functions is defined as:

$$\boldsymbol{W}\{K_0(X), I_0(X)\} = I_1(X)K_0(X) + K_1(X)I_0(X) = \frac{1}{X}\ , \quad \text{..... A. 44}$$

hence, β_2' can be easily obtained as:

$$\beta_2'(r_D, Z) = \frac{G_D I_0(X)}{Z^{3/2}} = G_D \frac{I_0\left(\sqrt{Z}r_D\right)}{Z}\ , \quad \text{..... A. 45}$$

and β_1' results in:

$$\beta_1'(r_D, Z) = -\frac{G_D K_0(X)}{Z^{3/2}} = \frac{G_D K_0\left(\sqrt{Z}r_D\right)}{Z}\ . \quad \text{..... A. 46}$$

Now, integrating[1] for β_1 and β_2 yields to:

$$\beta_1\left(\sqrt{Z}r_D\right) = -1.5708\ \frac{G_D r_D}{Z}\left[K_0\left(\sqrt{Z}r_D\right) L_{-1}\left(\sqrt{Z}r_D\right) + K_1\left(\sqrt{Z}r_D\right) L_0\left(\sqrt{Z}r_D\right)\right]\ . \quad \text{..... A. 47}$$

$$\beta_2\left(\sqrt{Z}r_D\right) = \frac{G_D r_D}{Z}\ {}_1\mathrm{F}_2\left(0.5, \{1,1.5\}, \frac{Z r_D^2}{4}\right)\ , \quad \text{..... A. 48}$$

where L_v are modified Struve functions and ${}_n\mathrm{F}_m$ are confluent hypergeometric functions. Therefore, the problem's solution in the Laplace space is:

$$\bar{P}_D(r_D, Z) = \alpha_1 I_0\left(\sqrt{Z}r_D\right) + \alpha_2 K_0\left(\sqrt{Z}r_D\right)$$
$$-1.5708\ \frac{G_D r_D}{Z}\left[K_0\left(\sqrt{Z}r_D\right) L_{-1}\left(\sqrt{Z}r_D\right) + K_1\left(\sqrt{Z}r_D\right) L_0\left(\sqrt{Z}r_D\right)\right] I_0\left(\sqrt{Z}r_D\right) +$$
$$\frac{G_D r_D}{Z}\ {}_1\mathrm{F}_2\left(0.5, \{1,1.5\}, \frac{Z r_D^2}{4}\right) K_0\left(\sqrt{Z}r_D\right)\ . \quad \text{... A. 49}$$

[1] Calculations performed with the use of Wolfram Mathematica.

To apply the boundary conditions, it is considered that the well's drainage area is much more larger than the wellbore radius. Hence, for the outer boundary:

$$\lim_{r_D\to\infty}\bar{P}_D=\lim_{r_D\to\infty}\Big[\alpha_1 I_0\big(\sqrt{Z}r_D\big)+\alpha_2 K_0\big(\sqrt{Z}r_D\big)$$

$$-1.5708\,\frac{G_D r_D}{Z}\big[K_0\big(\sqrt{Z}r_D\big)\,L_{-1}\big(\sqrt{Z}r_D\big)+\,K_1\big(\sqrt{Z}r_D\big)\,L_0\big(\sqrt{Z}r_D\big)\big]I_0\big(\sqrt{Z}r_D\big)$$

$$+\frac{G_D r_D}{Z}\;{}_1\mathrm{F}_2\left(0.5,\{1,1.5\},\frac{Z r_D^2}{4}\right)K_0\big(\sqrt{Z}r_D\big)\Big]=\lim_{r_D\to\infty}\big[\alpha_1 I_0\big(\sqrt{Z}r_D\big)\big]=0$$

for which $\alpha_1=0$; and letting $r_D\to 0$:

$$\lim_{r_D\to 0} r_D\frac{d\bar{P}_D}{dr_D}=\lim_{r_D\to 0} r_D\left[-\alpha_2\sqrt{Z}K_1\big(\sqrt{Z}r_D\big)+0.0236\frac{G_D}{Z}K_0\big(\sqrt{Z}r_D\big)\right]$$

$$=-\alpha_2+0.0236\frac{G_D}{Z}K_0\big(\sqrt{Z}r_D\big)=-\frac{1}{Z}-\frac{G_D}{Z}$$

and now valuating in $r_D=1$, it is obtained that

$$\alpha_2=\frac{1}{Z}+0.0236\frac{G_D}{Z}K_0\big(\sqrt{Z}\big)+\frac{G_D}{Z}=\frac{1}{Z}\big\{1+G_D\big[0.0236K_0\big(\sqrt{Z}\big)+1\big]\big\}\ .$$

Then, when substituting α_1 and α_2 into Eq. A. 49, the following equation is obtained:

$$\bar{P}_D(r_D,Z)=\frac{1}{Z}\big\{1+G_D\big[0.0236K_0\big(\sqrt{Z}\big)+1\big]\big\}K_0\big(\sqrt{Z}r_D\big)$$

$$-1.5708\,\frac{G_D r_D}{Z}\big[K_0\big(\sqrt{Z}r_D\big)\,L_{-1}\big(\sqrt{Z}r_D\big)+\,K_1\big(\sqrt{Z}r_D\big)\,L_0\big(\sqrt{Z}r_D\big)\big]I_0\big(\sqrt{Z}r_D\big)+ \qquad \text{... A. 50}$$

$$\frac{G_D r_D}{Z}\;{}_1\mathrm{F}_2\left(0.5,\{1,1.5\},\frac{Z r_D^2}{4}\right)K_0\big(\sqrt{Z}r_D\big)\ .$$

The full inversion of Eq. A. 50 requires the use of numerical methods (P.E. Schapery, Gaver-Stehfest or Fourier methods). However, to obtain a practical analytical solution, an asymptotic approach is made for long times (when $Z\to 0$):

$$\lim_{Z\to 0}\bar{P}_D\,(r_D,Z)=\lim_{Z\to 0}\left[\frac{1}{Z}\{1+G_D\big(0.0236K_0\big(\sqrt{Z}\big)+1\big)\}K_0\big(\sqrt{Z}r_D\big)\right.$$
$$-1.5708\,\frac{G_D r_D}{Z}\big[K_0\big(\sqrt{Z}r_D\big)\,L_{-1}\big(\sqrt{Z}r_D\big)+\,K_1\big(\sqrt{Z}r_D\big)\,L_0\big(\sqrt{Z}r_D\big)\big]I_0\big(\sqrt{Z}r_D\big)$$
$$\left.+\frac{G_D r_D}{Z}\;{}_1\mathrm{F}_2\,\left(0.5,\{1,1.5\},\frac{Z r_D^2}{4}\right)K_0\big(\sqrt{Z}r_D\big)\right]$$

which approximates to

$$\bar{P}_D(r_D,Z)\approx-\frac{1}{Z}\{1-G_D(0.0236\langle 0.5\ln|Z|+\ln|0.5|+\gamma\rangle+1+0.5236r_D)\}\langle 0.5\ln|Z|$$
$$+\ln|0.5r_D|+\gamma\rangle\ ,$$

or

$$\bar{P}_D(r_D,Z)=-\frac{1}{Z}\{1-G_D(0.0236\langle\ln|0.5|+\gamma\rangle+1+0.5236r_D)\}\langle 0.5\ln|Z|+\ln|0.5r_D|+\gamma\rangle$$
$$+\frac{0.0118G_D\ln|Z|}{Z}\langle\ln|0.5r_D|+\gamma\rangle+\frac{0.0059G_D\ln|Z|^2}{Z}\ ,$$

and directly inverting the terms:

$$p_{D_{NN}}(r_D,Z)=\{1-G_D(0.0236\langle\ln|0.5|+\gamma\rangle+1+0.5236r_D)\}\langle 0.5\ln\left|t_{D_{NN}}/r_D^2\right|+0.40455\rangle$$
$$-0.0118G_D\langle\ln\left|t_{D_{NN}}\right|+\gamma\rangle\langle\ln|0.5r_D|+\gamma\rangle$$
$$+0.0059G_D\left[\ln\left|t_{D_{NN}}\right|^2+2\gamma\ln\left|t_{D_{NN}}\right|+\gamma^2-\frac{\pi^2}{6}\right]$$

which rearranges into:

$$p_D\big(r_D,t_{D_{NN}}\big)=0.5\ln\left|\frac{t_{D_{NN}}}{r_D^2}\right|+0.40455$$
$$+G_D\left\{-(0.997264016+0.5236r_D)\langle 0.5\ln|r_D^2|-0.40455\rangle\right.$$
$$-0.5(0.99045287115418+0.5236r_D)\ln\left|t_{D_{NN}}\right|$$
$$\left.+0.0059\ln\left|t_{D_{NN}}\right|^2-0.007739361243949452\right\}\ ,\qquad \text{... A. 51}$$

where at $r_D = 1$ can be approximated to

$$p_{D_{NN}}(1, t_D) \approx -\frac{1}{2} E_i\left(-\frac{0.25}{t_{D_{NN}}}\right) + G_D \delta\left(t_{D_{NN}}\right)\omega \ , \quad \text{..... A. 52}$$

where $\omega = 0.0019 \ln\left|t_{D_{NN}}\right|^2 - 0.0072 \ln\left|t_{D_{NN}}\right| + 0.6173.$

Appendix B

Penetration distance for a Bingham plastic fluid

Under steady state conditions, the flow problem of a Bingham plastic fluid can be represented as:

$$\frac{d}{dr_D}\left(r_D \frac{dp_{D_{NN}}}{dr_D}\right) = -G_D \ , \quad \text{..... B. 1}$$

$$r_D \frac{\partial p_{D_{NN}}}{\partial r_D}(r_D = 1) = -1 - G_D \ , \quad \text{..... B. 2}$$

$$p_{D_{NN}}(r_D = \delta_D) = 0 \ . \quad \text{..... B. 3}$$

The solution of this problem can be easily obtained by direct integration twice:

$$p_{D_{NN}}(r_D) = -G_D r_D + A \ln|r_D| + B \ , \quad \text{..... B. 4}$$

and applying boundary conditions:

$$p_{D_{NN}}(\delta_D) = -G_D \delta_D + A \ln|\delta_D| + B = 0, \qquad B = G_D \delta_D - A \ln|\delta_D| \ .$$

$$r_D \frac{dp_{D_{NN}}}{dr_D}(r_D = 1) = -G_D + A = -1 - G_D \ , \qquad A = -1 \ .$$

Hence, the resulting expression is

$$p_{D_{NN}}(r_D) = -G_D r_D - \ln|r_D| + G_D \delta_D + \ln|\delta_D| \ . \quad \text{..... B. 5}$$

Now, evaluating from the wellbore's radius ($r_D = 1$) and comparing with Eq. 5. 17 at large times ($t_{D_{NN}} \gg 25$), it yields to:

$$\ln|\delta_D| = 0.5 \ln\left|\xi t_{D_{NN}} \exp(0.8091 + 2G_D)\right| \ ,$$

or

$$\delta_D = \sqrt{(1 - G_D) t_{D_{NN}} \exp(0.8091 + 2G_D)} \ . \quad \text{.....} \quad \text{B. 6}$$

Appendix C

Reservoir simulator for Bingham plastic fluids

Considering the Bingham plastic problem, a fully implicit linear simulator was developed for a central node finite difference scheme. For it, the logarithmic transformation was applied, **Figure C.1**:

$$x = \ln|r_D|\,, \qquad r_D = e^x \;, \quad \text{..... C. 1}$$

and the resulting problem is

$$\frac{\partial^2 p_D}{\partial x^2} + e^x G_D = e^{2x}\frac{\partial p_D}{\partial t_D} \;, \quad \text{..... C. 2}$$

$$p_{D_{NN}}(X,0) = 0 \;, \quad \text{..... C. 3}$$

$$\left(\frac{\partial p_{D_{NN}}}{\partial x}\right)_{x=0} = -1 - G_D \qquad t_{D_{NN}} > 0 \;, \quad \text{..... C. 4}$$

$$\left(\frac{\partial p_{D_{NN}}}{\partial x}\right)_{x=x_e} = 0 \qquad t_{D_{NN}} > 0 \;. \quad \text{..... C. 5}$$

Now, applying central differences to the derivatives in Eqs. C. 1 to C. 4:

$$\frac{\partial^2 p_D}{\partial x^2} \approx \frac{p_{i-1}^{m+1} - 2p_i^{m+1} + p_{i-1}^{m+1}}{\Delta x^2} \;, \quad \text{..... C. 6}$$

$$\frac{\partial p_D}{\partial t_D} \approx \frac{p_i^{m+1} - p_i^m}{\Delta t} \;, \quad \text{..... C. 7}$$

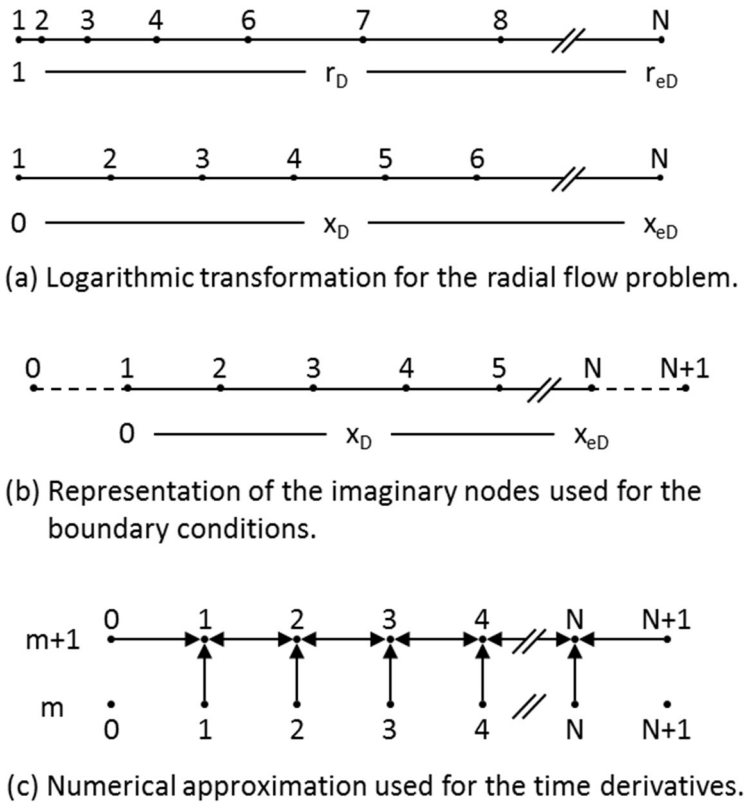

Figure C. 1. Schematization of the numerical discretization used for radial flow.

the resulting model is

$$p_{i-1}^{m+1} - (2 + \lambda_i)p_i^{m+1} + p_{i-1}^{m+1} = -\omega_i G_D - \lambda_i p_i^m \ , \quad \text{..... C. 8}$$

where

$$\lambda_i = \frac{\Delta x^2}{2\Delta t} e^{2\Delta x(i-1)} \ , \qquad \omega_i = \Delta x^2 e^{\Delta x(i-1)} \ . \quad \text{..... C. 9}$$

Similarly, considering that

$$\frac{\partial p_D}{\partial x} \approx \frac{p_{i+1} - p_{i-1}}{2\Delta x} \ , \quad \text{..... C. 10}$$

the boundary conditions are expressed as

$$\left.\frac{p_{i+1}-p_{i-1}}{2\Delta x}\right|_{x=0} = -1 - G_D \ , \quad \text{..... C. 11}$$

$$\left.\frac{p_{i+1}-p_{i-1}}{2\Delta x}\right|_{x=x_e} = 0 \ . \quad \text{..... C. 12}$$

Finally, the numerical model is:

in $x = 0$ for $i = 1$

$$-(2+\lambda_1)p_1^{m+1} + 2p_2^{m+1} = -2\Delta x + G_D(2\Delta x - \omega_1) - \lambda_1 p_1^m \ , \quad \text{..... C. 13}$$

in $x = x_e$ for $i = N$

$$2p_{N-1}^{m+1} - (2+\lambda_N)p_N^{m+1} = -G_D(2\Delta x + \omega_N) - \lambda_N p_N^m \ , \quad \text{..... C. 14}$$

in general for $1 < i < N$

$$p_{i-1}^{m+1} - (2+\lambda_i)p_i^{m+1} + p_{i+1}^{m+1} = -\omega_i G_D - \lambda_i p_i^m \ . \quad \text{..... C. 15}$$

Here it is seen that the resulting model is a tridiagonal system with:

$$a_1 = 0 \ , \qquad a_i = 1 \ , \qquad a_N = 2 \ ,$$

$$b_i = -(2+\lambda_i) \ ,$$

$$c_1 = 2 \ , \qquad c_i = 1 \ , \qquad c_N = 0 \ ,$$

$$d_1 = -2\Delta x + G_D(2\Delta x - \omega_1) - \lambda_1 p_1^m \ , \qquad d_i = -\omega_i G_D - \lambda_i p_i^m \ ,$$
$$d_N = -G_D(2\Delta x + \omega_N) - \lambda_N p_N^m \ .$$

For its solution the Thomas method is suggested.